

Introduction to Numerical Hydrodynamics

Bernd Freytag, Naples

January 24, 2010

Contents

1	Introduction of the equations of fluid dynamics	7
1.1	Presentation of the Euler equations	7
1.1.1	The Euler equations in differential form (vectors)	7
1.1.2	The Euler equations in differential form (components)	7
1.1.3	The solution of the Euler equations	7
1.1.4	The prototype numerical solution of the Euler equations	7
1.2	Derivation of the Euler equations	8
1.2.1	Possible basic quantities	8
1.2.2	Choice of basic quantities	8
1.2.3	Fluxes through surface	9
1.2.4	Changes of the conserved quantities	9
1.2.5	Euler equations in integral form	9
1.2.6	Euler equations: from integral to differential form I	9
1.2.7	Euler equations: from integral to differential form II	10
1.3	Extensions of the Euler equations	10
1.3.1	Hydrodynamics equations including viscosity	10
1.3.2	Hydrodynamics equations including gravity	10
1.3.3	Hydrodynamics equations including magnetic fields	11
1.3.4	Hydrodynamics equations including radiation	11
1.4	Radiation hydrodynamics of stellar atmospheres	11
1.4.1	Conditions in stellar atmospheres	11
1.4.2	Stationary case: assumptions	12
1.4.3	Stationary case: results	12
1.4.4	Static case	12
1.4.5	Coupling of radiation transport and hydrodynamics	12
1.5	Euler equations as hyperbolic system	13
1.5.1	1D Euler equations in conservation form	13
1.5.2	Quasi-linear system	13
1.5.3	Hyperbolic system	13
1.5.4	Eigenvalues for the Euler equations	14
2	The one-dimensional linear advection equation	15
2.1	Introduction of the linear advection equation	15
2.1.1	Linear advection as special case: density and momentum	15
2.1.2	Linear advection as special case: total energy	15
2.1.3	Linear advection as special case	15
2.1.4	Analytic solution of the linear advection equation	15
2.1.5	Solution along characteristic curves	16
2.2	Naive numerics: discretization attempts	16
2.2.1	Simple ODE: discretization	16
2.2.2	Simple ODE: examples	16
2.2.3	Simple ODE: remarks	17
2.2.4	Parabolic PDE: heat equation	17
2.2.5	Parabolic PDE: discretization	17
2.2.6	Parabolic PDE: stability	18
2.2.7	Parabolic PDE: example	18
2.2.8	Linear advection equation: discretization	18
2.2.9	Linear advection equation: crash	19
2.2.10	Linear advection equation: the lesson	19
2.3	Basic concepts	19
2.3.1	Discretization in space: wishlist	19
2.3.2	Discretization in space by finite differences	20

2.3.3	Discretization in space by finite volumes	20
2.3.4	Discretization in space by other methods	20
2.3.5	Discretization in space: grids	21
2.3.6	Integral form and weak solution	21
2.3.7	Integral form and flux centering	21
2.3.8	Centering of quantities, fluxes, and differences	22
2.3.9	Update formula in conservation form	22
2.3.10	Stencil diagrams	22
2.3.11	Stencil diagrams: spatial centering	23
2.3.12	Stencil diagrams: centering in time	23
2.3.13	CFL condition	24
2.3.14	Truncation error	24
2.3.15	Consistency – stability – convergence	24
2.3.16	Derivations of donor cell scheme	25
2.3.17	Further concepts	25
2.4	Examples	25
2.4.1	Parameter of the following examples	25
2.4.2	Naive FTCS scheme	26
2.4.3	Implicit centered scheme	26
2.4.4	BTCS scheme	26
2.4.5	Donor cell (FTBS) scheme	27
2.4.6	FTFS scheme	27
2.4.7	Lax-Friedrichs scheme	28
2.4.8	Lax-Wendroff scheme	28
2.4.9	Beam-Warming scheme	28
2.4.10	Fromm scheme	29
2.5	Analysis of schemes	29
2.5.1	Overshoot	29
2.5.2	Artificial viscosity	30
2.5.3	Modified equation for the FTFS scheme I	31
2.5.4	Modified equation for the FTFS scheme II	31
2.5.5	Modified equation for the FTBS scheme	31
2.5.6	Linear stability analysis of original PDE	31
2.5.7	Linear stability analysis: use	32
2.5.8	Linear stability analysis of naive FTCS scheme	32
2.5.9	Linear stability analysis of donor cell (FTBS) scheme	32
2.5.10	Linear stability analysis: remarks	33
2.6	Non-linear schemes	33
2.6.1	Godunov’s idea	33
2.6.2	Monotonicity	33
2.6.3	Flux of PLM schemes	34
2.6.4	Examples: PLM: slopes with linear parameter dependence	34
2.6.5	PLM: slope-limiter	34
2.6.6	PLM scheme with Minmod slope-limiter	34
2.6.7	PLM scheme with vanLeer slope-limiter	35
2.6.8	PLM scheme with Superbee slope-limiter	36
2.6.9	PPM scheme	36
2.6.10	WENO scheme	36
2.6.11	Scheme with Superbee slope, only boundary value used	36
2.6.12	Further improvements	37

3	Non-linear advection: Burgers' equation	38
3.1	Introduction of Burgers' equation	38
3.1.1	Viscous and inviscid Burgers' equation	38
3.1.2	Solution along characteristic curves	38
3.1.3	Compression waves and shocks	38
3.1.4	Shock speed I	39
3.1.5	Shock speed II	39
3.1.6	Expansion waves	39
3.1.7	Similarity solutions I	40
3.1.8	Similarity solutions II	40
3.1.9	Classification of Riemann problems	40
3.2	Numerical examples	41
3.2.1	Velocity at cell boundary	41
3.2.2	Flux-splitting	41
3.2.3	Example: small-amplitude wave	41
3.2.4	Example: Gaussian and conservativity	41
3.2.5	Lax-Wendroff theorem	42
3.2.6	Example: step-function and conservativity	42
3.2.7	Example: expansion shock and rarefaction fan	43
3.2.8	Entropy production by artificial viscosity	43
3.2.9	Entropy fix	44
3.2.10	Concepts from the linear world	44
3.2.11	Transformation of shock speed formula	44
3.2.12	Second-order extension of flux formula	45
4	One-dimensional non-linear hydrodynamics	46
4.1	New Difficulties	46
4.1.1	A coupled non-linear system	46
4.1.2	Positivity of density	46
4.1.3	Positivity of pressure	46
4.1.4	Where is upwind?	46
4.2	The Riemann problem for the 1D Euler equations	47
4.2.1	The Riemann problem	47
4.2.2	Rankine-Hugoniot conditions	47
4.2.3	Example: Sod shock tube	47
4.2.4	Jumps in the solution of the Sod shock tube problem	48
4.3	Riemann solvers	48
4.3.1	Godunov-type schemes	48
4.3.2	Riemann solvers and higher-order schemes	48
4.4	Approximate (linear) Riemann solvers	49
4.4.1	Linearized flux	49
4.4.2	Linearized Riemann solver	49
4.4.3	Examples of schemes	49
4.4.4	Example: Sod shock tube with Roe solver, constant	50
4.4.5	Example: Sod shock tube with Roe solver, Minmod slope	50
4.4.6	Example: Sod shock tube with Roe solver, vanLeer slope	51
4.4.7	Example: Sod shock tube with Roe solver, Superbee slope	51
4.4.8	Example: Sod shock tube with Roe solver, PP reconstruction	51
4.5	Alternative concepts	51

5 Applications	53
5.1 Composing operators	53
5.1.1 Operator adding versus splitting	53
5.1.2 Godunov versus Strang operator splitting	53
5.1.3 Steady-state solutions with operator adding or splitting	53
5.1.4 Linear stability of operator adding or splitting	54
5.1.5 Going multi-dimensional	54
5.2 Coupling of hydrodynamics and radiation transport	54
5.2.1 Coupling	54
5.2.2 Stability requirements	55
5.2.3 Approximations	55
5.3 Improvements	55
5.3.1 Non-Cartesian and/or refined grids	55
5.3.2 Optimization strategies	55
A Nomenclature	57
A.1 Quantities	57
A.2 Vector notation	57
B Schedule	58
C References	59
C.1 Lecture Notes	59
C.2 Books	59
C.3 Articles	60
C.4 Hydrodynamic codes	60

List of Figures

1	First order integration of ODE	17
2	Heat equation	18
3	Heat equation: spikes	18
4	Linear advection: crash	19
5	Flux centering	21
6	Stencil diagram	22
7	Stencil diagrams: spatial centering	23
8	Stencil diagrams: time-centering	23
9	Naive scheme: stencil diagram and test	26
10	Implicit scheme: stencil diagram and test	26
11	BTCS scheme: stencil diagram and test	27
12	Stencil, example for donor cell scheme	27
13	Stencil, example for FTFS scheme	28
14	Stencil, example for Lax-Friedrichs scheme	28
15	Stencil, example for Lax-Wendroff scheme	29
16	Stencil, example for Beam-Warming scheme	29
17	Stencil, example for Fromm scheme	30
18	Example for Lax-Wendroff and Beam-Warming scheme	30
19	Stencil, example for PLM/Minmod scheme	35
20	Stencil, example for PLM/vanLeer scheme	35
21	Stencil, example for PLM/Superbee scheme	36
22	Stencil, example for PPM scheme	36
23	Stencil, example for WENO scheme	37
24	Stencil, example for sharpened PLM/Superbee scheme	37
25	Jump	39
26	Riemann problems for Burgers equation	40
27	Shock from small-amplitude wave	42
28	Non-conservative scheme	42
29	Non-conservative scheme	43
30	Expansion shock	43
31	Sod shock tube	47
32	Many Riemann problems	48
33	Sod shock tube, constant	50
34	Sod shock tube, Minmod	50
35	Sod shock tube, vanLeer	51
36	Sod shock tube, Superbee	51
37	Sod shock tube, PP	52

List of Tables

1	Symbols and descriptions for quantities	57
2	Vector notation	57

1 Introduction of the equations of fluid dynamics

1.1 Presentation of the Euler equations

1.1.1 The Euler equations in differential form (vectors)

The Euler equations in differential conservation form in vector notation are

$$\begin{aligned} \frac{\partial \rho}{\partial t} + \nabla \cdot (\rho \mathbf{v}) &= 0 \\ \frac{\partial \rho \mathbf{v}}{\partial t} + \nabla \cdot (\rho \mathbf{v} : \mathbf{v} + P \bar{\mathbf{1}}) &= \mathbf{0} \\ \frac{\partial \rho e_{\text{ik}}}{\partial t} + \nabla \cdot ([\rho e_{\text{ik}} + P] \mathbf{v}) &= 0 \end{aligned} \quad (1)$$

They describe the inviscid flow of density ρ , momentum $\rho \mathbf{v}$, and total energy ρe_{ik} , with

\mathbf{v} velocity vector

e_{ik} total (internal + kinetic) energy per mass unit

P pressure

$\bar{\mathbf{1}}$ unity tensor .

1.1.2 The Euler equations in differential form (components)

The Euler equations in differential conservation form, split into components, are

$$\begin{aligned} \frac{\partial}{\partial t} \rho + \frac{\partial}{\partial x} (\rho v_x) + \frac{\partial}{\partial y} (\rho v_y) + \frac{\partial}{\partial z} (\rho v_z) &= 0 \\ \frac{\partial}{\partial t} \begin{pmatrix} \rho v_x \\ \rho v_y \\ \rho v_z \end{pmatrix} + \frac{\partial}{\partial x} \begin{pmatrix} \rho v_x v_x + P \\ \rho v_y v_x \\ \rho v_z v_x \end{pmatrix} + \frac{\partial}{\partial y} \begin{pmatrix} \rho v_x v_y \\ \rho v_y v_y + P \\ \rho v_z v_y \end{pmatrix} + \frac{\partial}{\partial z} \begin{pmatrix} \rho v_x v_z \\ \rho v_y v_z \\ \rho v_z v_z + P \end{pmatrix} &= \begin{pmatrix} 0 \\ 0 \\ 0 \end{pmatrix} \\ \frac{\partial}{\partial t} \rho e_{\text{ik}} + \frac{\partial}{\partial x} ([\rho e_{\text{ik}} + P] v_x) + \frac{\partial}{\partial y} ([\rho e_{\text{ik}} + P] v_y) + \frac{\partial}{\partial z} ([\rho e_{\text{ik}} + P] v_z) &= 0 . \end{aligned} \quad (2)$$

It is a system of first-order partial differential equations (PDEs).

1.1.3 The solution of the Euler equations

The task is now: Find a solution for Eq. (2) for given initial conditions

$$(\rho, \rho \mathbf{v}, \rho e_{\text{ik}}) (\mathbf{x}, t_0) , \quad (3)$$

boundary conditions

$$(\rho, \rho \mathbf{v}, \rho e_{\text{ik}}) (\mathbf{x}_{\text{boundaries}}, t) , \quad (4)$$

and material function (equation of state)

$$P = P(\rho, e_i) \quad (5)$$

with

$$e_i = e_{\text{ik}} - \frac{1}{2} \mathbf{v} \cdot \mathbf{v} . \quad (6)$$

1.1.4 The prototype numerical solution of the Euler equations

The hydrodynamics equations (1) or (2) can be put into the form

$$\frac{\partial}{\partial t} (\rho, \rho \mathbf{v}, \rho e_{\text{ik}}) = f(\rho, \rho \mathbf{v}, \rho e_{\text{ik}}) \quad (7)$$

where the function f contains the terms with the spatial derivatives.

Idea:

1. take initial state $(\rho, \rho\mathbf{v}, \rho e_{ik})(\mathbf{x}, t_0)$ given on a grid
2. compute \mathbf{v} , e_i , and P
3. compute the spatial derivatives to get the right-hand side of Eq. (7)
4. get a small change of $(\rho, \rho\mathbf{v}, \rho e_{ik})$ in time
5. update $(\rho, \rho\mathbf{v}, \rho e_{ik})$
6. restart at 2

There 1000 ways how this can go wrong...

1.2 Derivation of the Euler equations

1.2.1 Possible basic quantities

What do we need to describe a – simple – fluid locally?

- **Macroscopic** bulk velocity \mathbf{v} (or momentum $\rho\mathbf{v}$)
- Two thermodynamic quantities, e.g.
 - temperature T and pressure P
 - or mass density ρ and internal energy e_i

All quantities depend on space \mathbf{x} and time t . We assume

- LTE: two thermodynamic quantities are sufficient to describe the local **microscopic** state of the fluid completely: element composition, ionization, occupation numbers, microscopic velocity distribution,
- we do not need to look at the **atomic** level: we have a continuous fluid.

1.2.2 Choice of basic quantities

We choose the **conserved variables**

- density ρ ,
- momentum $\rho\mathbf{v}$,
- total energy e_{ik}

as basic quantities, because they have

- no source terms (we ignore gravity here),
- simpler transport properties

rather than e.g. the **primitive variables**

- density ρ ,
- velocity \mathbf{v} ,
- pressure P .

1.2.3 Fluxes through surface

Fluxes through surface element dA with normal vector $\hat{\mathbf{n}}$:

Mass transport \rightarrow change of mass per time:

$$\rho \mathbf{v} \cdot \hat{\mathbf{n}} dA \quad (8)$$

Momentum transport and acceleration by pressure force along surface normal \rightarrow change of momentum per time

$$[\rho \mathbf{v} : \mathbf{v} \hat{\mathbf{n}} + P \hat{\mathbf{n}}] dA \quad (9)$$

Energy transport and work done by pressure \rightarrow change of total energy per time

$$[\rho e_{ik} + P] \mathbf{v} \cdot \hat{\mathbf{n}} dA \quad (10)$$

Shear forces (friction) are ignored.

There are no torsional forces (only relevant in solids).

1.2.4 Changes of the conserved quantities

Without source terms the only change between time t_1 and t_0 to the amount of a conserved variable inside a volume V comes from the flux through its surface ∂V .

Integrating Eqs. (8) to (10) over that surface and time thus gives

$$\int_V \rho(\mathbf{x}, t_1) dV - \int_V \rho(\mathbf{x}, t_0) dV = - \int_{t_0}^{t_1} \oint_{\partial V} \rho \mathbf{v} \cdot \hat{\mathbf{n}} dA dt \quad (11)$$

$$\int_V \rho \mathbf{v}(\mathbf{x}, t_1) dV - \int_V \rho \mathbf{v}(\mathbf{x}, t_0) dV = - \int_{t_0}^{t_1} \oint_{\partial V} [\rho \mathbf{v} : \mathbf{v} + P \bar{\mathbf{I}}] \hat{\mathbf{n}} dA dt \quad (12)$$

$$\int_V \rho e_{ik}(\mathbf{x}, t_1) dV - \int_V \rho e_{ik}(\mathbf{x}, t_0) dV = - \int_{t_0}^{t_1} \oint_{\partial V} [\rho e_{ik} + P] \mathbf{v} \cdot \hat{\mathbf{n}} dA dt \quad (13)$$

The unity tensor $\bar{\mathbf{I}}$ has been squeezed in,

$$P \hat{\mathbf{n}} = P \bar{\mathbf{I}} \hat{\mathbf{n}} . \quad (14)$$

1.2.5 Euler equations in integral form

After a slight rearrangement we get the **Euler equations in integral form**:

$$\begin{aligned} \int_V [\rho(\mathbf{x}, t_1) - \rho(\mathbf{x}, t_0)] dV &+ \int_{t_0}^{t_1} \oint_{\partial V} \rho \mathbf{v} \cdot \hat{\mathbf{n}} dA dt &= 0 \\ \int_V [\rho \mathbf{v}(\mathbf{x}, t_1) - \rho \mathbf{v}(\mathbf{x}, t_0)] dV &+ \int_{t_0}^{t_1} \oint_{\partial V} [\rho \mathbf{v} : \mathbf{v} + P \bar{\mathbf{I}}] \hat{\mathbf{n}} dA dt &= \mathbf{0} \\ \int_V [\rho e_{ik}(\mathbf{x}, t_1) - \rho e_{ik}(\mathbf{x}, t_0)] dV &+ \int_{t_0}^{t_1} \oint_{\partial V} [\rho e_{ik} + P] \mathbf{v} \cdot \hat{\mathbf{n}} dA dt &= 0 \end{aligned} \quad (15)$$

There is a close correspondence to the Euler equations in differential form (1). Note however, that in the integral form there are no derivatives.

1.2.6 Euler equations: from integral to differential form I

To transform the mass transport equation into differential form the first line of Eq. (15) is divided by $(t_1 - t_0)$,

$$\int_V \frac{\rho(\mathbf{x}, t_1) - \rho(\mathbf{x}, t_0)}{t_1 - t_0} dV + \frac{1}{t_1 - t_0} \int_{t_0}^{t_1} \oint_{\partial V} \rho \mathbf{v} \cdot \hat{\mathbf{n}} dA dt = 0 . \quad (16)$$

Taking the limes $t_1 \rightarrow t_0$ and assuming that the derivative $\frac{\partial \rho}{\partial t}$ exists for all \mathbf{x} we get

$$\int_V \frac{\partial \rho}{\partial t} dV + \oint_{\partial V} \rho \mathbf{v} \cdot \hat{\mathbf{n}} dA = 0 . \quad (17)$$

Now, the **Gauß theorem** is applied (assuming that the divergence $\nabla \cdot \rho \mathbf{v}$ does exist) to transform the surface integral into a volume integral. We get

$$\int_V \frac{\partial \rho}{\partial t} dV + \int_V \nabla \cdot \rho \mathbf{v} dV = 0 . \quad (18)$$

1.2.7 Euler equations: from integral to differential form II

Merging the two integrals gives

$$\int_V \left(\frac{\partial \rho}{\partial t} + \nabla \cdot \rho \mathbf{v} \right) dV = 0 . \quad (19)$$

Because this is true for all (even small) volumes we conclude that the integrand has to be zero and get the differential form of the mass transport equation,

$$\frac{\partial \rho}{\partial t} + \nabla \cdot \rho \mathbf{v} = 0 . \quad (20)$$

This works the same for the energy equation and requires only a generalization of the Gauß theorem to be applicable to the momentum equation.

1.3 Extensions of the Euler equations

1.3.1 Hydrodynamics equations including viscosity

The **viscous** hydrodynamics equations are

$$\begin{aligned} \frac{\partial \rho}{\partial t} + \nabla \cdot (\rho \mathbf{v}) &= 0 \\ \frac{\partial \rho \mathbf{v}}{\partial t} + \nabla \cdot (\rho \mathbf{v} : \mathbf{v} - \bar{\bar{\mathbf{T}}}) &= \mathbf{0} \\ \frac{\partial \rho e_{\text{ik}}}{\partial t} + \nabla \cdot ([\rho e_{\text{ik}} - \bar{\bar{\mathbf{T}}}] \mathbf{v}) &= 0 \end{aligned} \quad (21)$$

with the **stress tensor** $\bar{\bar{\mathbf{T}}}$ (including a term for the gas pressure)

$$\bar{\bar{\mathbf{T}}} = -P \bar{\mathbf{1}} + \mu \left\{ [\nabla : \mathbf{v} + (\nabla : \mathbf{v})^{\text{T}}] - \frac{2}{3} \nabla \cdot \mathbf{v} \bar{\mathbf{1}} \right\} \quad (22)$$

depending on the **dynamic viscosity** μ .

Note: via $\bar{\bar{\mathbf{T}}}$ Eq. (21) contains second derivatives.

1.3.2 Hydrodynamics equations including gravity

The Euler equations with **gravity** are

$$\begin{aligned} \frac{\partial \rho}{\partial t} + \nabla \cdot (\rho \mathbf{v}) &= 0 \\ \frac{\partial \rho \mathbf{v}}{\partial t} + \nabla \cdot (\rho \mathbf{v} : \mathbf{v} + P \bar{\mathbf{1}}) &= -\rho \nabla \Phi \\ \frac{\partial \rho e_{\text{ikg}}}{\partial t} + \nabla \cdot ([\rho e_{\text{ikg}} + P] \mathbf{v}) &= 0 \end{aligned} \quad (23)$$

with the **gravitational potential** Φ . The total energy e_{ikg} now contains a contribution due to the potential,

$$e_{\text{ikg}} = e_i + \frac{1}{2} \mathbf{v} \cdot \mathbf{v} + \Phi . \quad (24)$$

Note: the momentum equation now contains a true **source term**.

1.3.3 Hydrodynamics equations including magnetic fields

The equations of **ideal magneto-hydrodynamics** (MHD) are

$$\begin{aligned}
\frac{\partial \rho}{\partial t} + \nabla \cdot (\rho \mathbf{v}) &= 0 \\
\frac{\partial \rho \mathbf{v}}{\partial t} + \nabla \cdot (\rho \mathbf{v} \cdot \mathbf{v} + P \bar{\mathbb{I}} - \bar{\mathbb{T}}_{\text{mag}}) &= \mathbf{0} \\
\frac{\partial \mathbf{B}}{\partial t} + \nabla \cdot (\mathbf{v} \cdot \mathbf{B} - \mathbf{B} \cdot \mathbf{v}) &= \mathbf{0} \\
\frac{\partial \rho e_{\text{ikb}}}{\partial t} + \nabla \cdot ([\rho e_{\text{ikb}} + P - \bar{\mathbb{T}}_{\text{mag}}] \mathbf{v}) &= 0
\end{aligned} \tag{25}$$

with the **magnetic field** \mathbf{B} (with $\nabla \cdot \mathbf{B} = 0$) and the **Maxwell stress tensor** $\bar{\mathbb{T}}_{\text{mag}}$

$$\bar{\mathbb{T}}_{\text{mag}} = -\frac{1}{2} \mathbf{B} \cdot \mathbf{B} \bar{\mathbb{I}} + \mathbf{B} : \mathbf{B} . \tag{26}$$

The total energy e_{ikb} now contains a contribution from the magnetic field,

$$e_{\text{ikb}} = e_{\text{i}} + \frac{1}{2} \mathbf{v} \cdot \mathbf{v} + \frac{1}{2} \mathbf{B} \cdot \mathbf{B} / \rho . \tag{27}$$

1.3.4 Hydrodynamics equations including radiation

The hydrodynamics equations including **radiative terms** are

$$\begin{aligned}
\frac{\partial \rho}{\partial t} + \nabla \cdot (\rho \mathbf{v}) &= 0 \\
\frac{\partial \rho \mathbf{v}}{\partial t} + \nabla \cdot (\rho \mathbf{v} \cdot \mathbf{v} + P \bar{\mathbb{I}} + \bar{\mathbb{P}}_{\text{rad}}) &= \mathbf{0} \\
\frac{\partial \rho e_{\text{ik}}}{\partial t} + \nabla \cdot ([\rho e_{\text{ik}} + P] \mathbf{v} + \mathbf{F}_{\text{rad}}) &= 0
\end{aligned} \tag{28}$$

where the **radiative energy flux** \mathbf{F}_{rad} and the **radiation pressure** $\bar{\mathbb{P}}_{\text{rad}}$ are computed from the intensity $I_\nu(\mathbf{x}, \hat{\mathbf{n}}, \nu)$ as (c_1 : speed of light, ν : frequency)

$$\mathbf{F}_{\text{rad}}(\mathbf{x}) = \int_0^\infty \oint_\Omega \hat{\mathbf{n}} I_\nu(\mathbf{x}, \hat{\mathbf{n}}, \nu) d\omega d\nu \tag{29}$$

$$\bar{\mathbb{P}}_{\text{rad}}(\mathbf{x}) = \frac{1}{c_1} \int_0^\infty \oint_\Omega \hat{\mathbf{n}} : \hat{\mathbf{n}} I_\nu(\mathbf{x}, \hat{\mathbf{n}}, \nu) d\omega d\nu . \tag{30}$$

1.4 Radiation hydrodynamics of stellar atmospheres

1.4.1 Conditions in stellar atmospheres

Flows in stellar atmospheres can be characterized by

- outer “boundary” of star: energy from the interior is radiated into space
- dominant stratification: “essentially 1D”
- transition region between optically thick and thin regime
- low viscosity (large Reynolds numbers)
- flow speeds typically near sonic (Mach numbers not far below 1)
- magnetic fields can play a role – in some cases

Ignore magnetic fields in Eq. (25) and viscous effects from Eq. (21).

Keep terms due to gravity as in Eq. (23) and the influence of radiation as in Eq. (28).

1.4.2 Stationary case: assumptions

Assumption: gravity in z direction (downward):

$$\Phi = gz \quad . \quad (31)$$

Assumption: quasi-stationarity (no trends, fluctuations allowed)

Averaging over t , x , and y gives

$$\frac{\partial}{\partial t} = 0, \quad \frac{\partial}{\partial x} = 0, \quad \frac{\partial}{\partial y} = 0 \quad . \quad (32)$$

1.4.3 Stationary case: results

The quasi-stationary combination of of Eq. (23) and Eq. (28) gives:

Mass transport: mass loss or infall (and, in fact, horizontal laminar flow)

$$\langle \rho v_z(z) \rangle = \text{const} \quad (33)$$

$$\langle \rho v_x(z) \rangle = \text{const}, \quad \langle \rho v_y(z) \rangle = \text{const} \quad (34)$$

Vertical momentum: turbulent, gas, radiation pressure + gravity \rightarrow pressure stratification

$$\frac{\partial}{\partial z} (\langle \rho v_z v_z \rangle + \langle P \rangle + \langle P_{\text{rad},z} \rangle) = -\langle \rho \rangle g \quad (35)$$

Energy flux: convective and radiative energy transport \rightarrow temperature stratification

$$\langle [\rho e_{\text{ikg}} + P] v_z \rangle + \langle F_{\text{rad},z} \rangle = \text{const} = F_* \quad (36)$$

1.4.4 Static case

Further assumption:

$$v_x = v_y = v_z = 0 \quad (37)$$

Result:

No mass loss

Hydrostatic pressure stratification:

$$\frac{\partial}{\partial z} (\langle P \rangle + \langle P_{\text{rad},z} \rangle) = -\langle \rho \rangle g \quad (38)$$

Stratification in radiative equilibrium:

$$\langle F_{\text{rad},z} \rangle = \text{const} = F_* \quad (39)$$

1.4.5 Coupling of radiation transport and hydrodynamics

Radiation transport \rightarrow hydrodynamics:

- affects energy and momentum
- non-local coupling
- possibly short radiative time-scale \rightarrow stiff terms

Hydrodynamics \rightarrow radiation transport:

- transport through complex 3D structures
- spatial fluctuations of ρ and $e_i \rightarrow$ fluctuations of opacities and source function
- Doppler shifts of wavelengths of lines

1.5 Euler equations as hyperbolic system

1.5.1 1D Euler equations in conservation form

The Euler equations (2) restricted to one spatial dimension,

$$\frac{\partial}{\partial t} \begin{pmatrix} \rho \\ \rho v \\ \rho e_{ik} \end{pmatrix} + \frac{\partial}{\partial x} \begin{pmatrix} \rho v \\ \rho v v + P \\ [\rho e_{ik} + P] v \end{pmatrix} = \begin{pmatrix} 0 \\ 0 \\ 0 \end{pmatrix} \quad (40)$$

have the form (**conservation form**)

$$\frac{\partial}{\partial t} \mathbf{q} + \frac{\partial}{\partial x} \mathbf{F}(\mathbf{q}) = \mathbf{0} \quad (41)$$

for the quantity vector \mathbf{q} with flux vector \mathbf{F} ,

$$\mathbf{q} = \begin{pmatrix} \rho \\ \rho v \\ \rho e_{ik} \end{pmatrix}, \quad \mathbf{F} = \begin{pmatrix} \rho v \\ \rho v v + P \\ [\rho e_{ik} + P] v \end{pmatrix}. \quad (42)$$

1.5.2 Quasi-linear system

In Eq. (41) we can compute the spatial derivative and get

$$\frac{\partial}{\partial t} \mathbf{q} + \bar{\bar{\mathbf{A}}} \frac{\partial}{\partial x} \mathbf{q} = \mathbf{0} \quad (43)$$

with the **Jacobian**

$$\bar{\bar{\mathbf{A}}} = \frac{\partial \mathbf{F}}{\partial \mathbf{q}}. \quad (44)$$

A system of partial differential equations in the form of Eq. (43) is called **quasi-linear** if

$$\bar{\bar{\mathbf{A}}} = \bar{\bar{\mathbf{A}}}(\mathbf{q}, x, t). \quad (45)$$

It is **linear** if $\bar{\bar{\mathbf{A}}}$ is constant.

1.5.3 Hyperbolic system

A linear system (43) of PDEs is called **hyperbolic** if $\bar{\bar{\mathbf{A}}}$ is **diagonalizable**, i.e., there exists a matrix $\bar{\bar{\mathbf{Q}}}$ with

$$\bar{\bar{\mathbf{A}}} = \bar{\bar{\mathbf{Q}}}^{-1} \bar{\bar{\mathbf{A}}} \bar{\bar{\mathbf{Q}}} \quad (46)$$

and $\bar{\bar{\mathbf{A}}}$ is in diagonal form (with real numbers on the diagonal: the eigenvalues of $\bar{\bar{\mathbf{A}}}$).

With the definition

$$\mathbf{q}' := \bar{\bar{\mathbf{Q}}}^{-1} \mathbf{q} \quad (47)$$

Eq. (43) gets the **characteristic form**

$$\frac{\partial}{\partial t} \mathbf{q}' + \bar{\bar{\mathbf{A}}} \frac{\partial}{\partial x} \mathbf{q}' = \mathbf{0}. \quad (48)$$

This is now a set of independent equations, each of the simple form

$$\frac{\partial}{\partial t} q'_i + \lambda_i \frac{\partial}{\partial x} q'_i = 0. \quad (49)$$

A quasi-linear system with $\bar{\bar{\mathbf{A}}}(\mathbf{q}, x, t)$ can be hyperbolic at point (\mathbf{q}, x, t) .

1.5.4 Eigenvalues for the Euler equations

For the 1D Euler equations (40) we get the **eigenvalues**

$$\begin{pmatrix} v \\ v + c \\ v - c \end{pmatrix}, \quad (50)$$

corresponding to the **flow** with velocity v and **two acoustic waves** travelling with sound speed $\pm c$ relative to the flow.

2 The one-dimensional linear advection equation

2.1 Introduction of the linear advection equation

2.1.1 Linear advection as special case: density and momentum

In a 1D flow described by Eq. (40) assuming $\frac{\partial P}{\partial x} = 0$ and $\frac{\partial v}{\partial x} = 0$ at $t = t_0$ gives for the mass

$$0 = \frac{\partial \rho}{\partial t} + \frac{\partial \rho v}{\partial x} \quad (51)$$

$$= \frac{\partial \rho}{\partial t} + v \frac{\partial \rho}{\partial x} , \quad (52)$$

for the momentum

$$0 = \frac{\partial \rho v}{\partial t} + \frac{\partial \rho v v}{\partial x} \quad (53)$$

$$= v \left(\frac{\partial \rho}{\partial t} + v \frac{\partial \rho}{\partial x} \right) + \rho \frac{\partial v}{\partial t} \quad (54)$$

$$= \rho \frac{\partial v}{\partial t} . \quad (55)$$

2.1.2 Linear advection as special case: total energy

For the total energy we get

$$0 = \frac{\partial \rho e_{ik}}{\partial t} + \frac{\partial \rho e_{ik} v}{\partial x} \quad (56)$$

$$= \frac{\partial}{\partial t} \left(\rho e_i + \frac{1}{2} \rho v^2 \right) + \frac{\partial}{\partial x} \left(\rho e_i v + \frac{1}{2} \rho v^2 v \right) \quad (57)$$

$$= \frac{1}{2} v^2 \left(\frac{\partial \rho}{\partial t} + v \frac{\partial \rho}{\partial x} \right) + \left(\frac{\partial \rho e_i}{\partial t} + \frac{\partial \rho e_i v}{\partial x} \right) \quad (58)$$

$$= \frac{\partial \rho e_i}{\partial t} + v \frac{\partial \rho e_i}{\partial x} . \quad (59)$$

2.1.3 Linear advection as special case

Finally, we get for the pressure $P(\rho e_i, \rho)$

$$\frac{\partial P}{\partial t} = \frac{\partial P}{\partial \rho e_i} \bigg|_{\rho} \frac{\partial \rho e_i}{\partial t} + \frac{\partial P}{\partial \rho} \bigg|_{\rho e_i} \frac{\partial \rho}{\partial t} \quad (60)$$

$$= \frac{\partial P}{\partial \rho e_i} \bigg|_{\rho} \left(-v \frac{\partial \rho e_i}{\partial x} \right) + \frac{\partial P}{\partial \rho} \bigg|_{\rho e_i} \left(-v \frac{\partial \rho}{\partial x} \right) \quad (61)$$

$$= -v \frac{\partial P}{\partial x} = 0 . \quad (62)$$

Thus, v and P are constant in space and time. The passive advection of ρ and ρe_i is described by the **linear advection equation**

$$\frac{\partial \rho}{\partial t} + v \frac{\partial \rho}{\partial x} = 0 \quad (63)$$

with $v = \text{const.}$

2.1.4 Analytic solution of the linear advection equation

For initial condition

$$\rho(x, t_0) = \rho_0(x) \quad (64)$$

the advection equation (63) has the **general solution**

$$\tilde{\rho}(x, t) = \rho_0(x - v[t - t_0]) . \quad (65)$$

Proof by checking: it fulfils the initial condition and

$$\frac{\partial \tilde{\rho}}{\partial t} + v \frac{\partial \tilde{\rho}}{\partial x} = \frac{d\rho_0}{dx} (-v) + v \frac{d\rho_0}{dx} 1 = 0 . \quad (66)$$

2.1.5 Solution along characteristic curves

For a quasi-linear PDE

$$\frac{\partial \rho}{\partial t} + v(\rho, x, t) \frac{\partial \rho}{\partial x} = 0 \quad (67)$$

a curve $c(t)$ with

$$\frac{dc}{dt} = v \quad (68)$$

or sometimes the corresponding map $\mathbb{R} \rightarrow \mathbb{R}^2: t \rightarrow (c(t), t)$ is called **characteristic curve** or **characteristic**. For the linear advection equation (63) these curves have the general form

$$c(t) = vt + x_0 . \quad (69)$$

Along $c(t)$ we get for a solution $\tilde{\rho}$ of Eq. (63)

$$\frac{d}{dt} \tilde{\rho}(c(t), t) = \frac{\partial \tilde{\rho}}{\partial t} + \frac{\partial \tilde{\rho}}{\partial x} \frac{dc}{dt} = \frac{\partial \tilde{\rho}}{\partial t} + v \frac{\partial \tilde{\rho}}{\partial x} = 0 . \quad (70)$$

The solution $\tilde{\rho}$ is **constant** along the characteristic $c(t)$.

2.2 Naive numerics: discretization attempts

2.2.1 Simple ODE: discretization

The simple ordinary differential equation (ODE)

$$\frac{dy}{dt} = -ay \quad (71)$$

with initial value

$$y(t_0) = y_0 \quad (72)$$

is of first order and linear with constant coefficient a . It has the obvious solution

$$y(t) = y_0 e^{-a(t-t_0)} . \quad (73)$$

For discrete time-steps

$$t^n = \Delta t n + t_0 \quad (74)$$

the straight-forward replacement $dt \rightarrow \Delta t$ gives the most simple discretization (**explicit Euler scheme**: approximation of y by a piecewise linear curve)

$$y^{n+1} = y^n - ay^n \Delta t . \quad (75)$$

2.2.2 Simple ODE: examples

Figure 1 shows examples for Eq. (75) for $a = 1$. The

$$\text{criterion for stability:} \quad \Delta t < 2/a \quad (76)$$

$$\text{criterion for positivity:} \quad \Delta t < 1/a \quad (77)$$

have a simple interpretation: Too large time-steps lead to conflicts with the actual curvature of the solution.

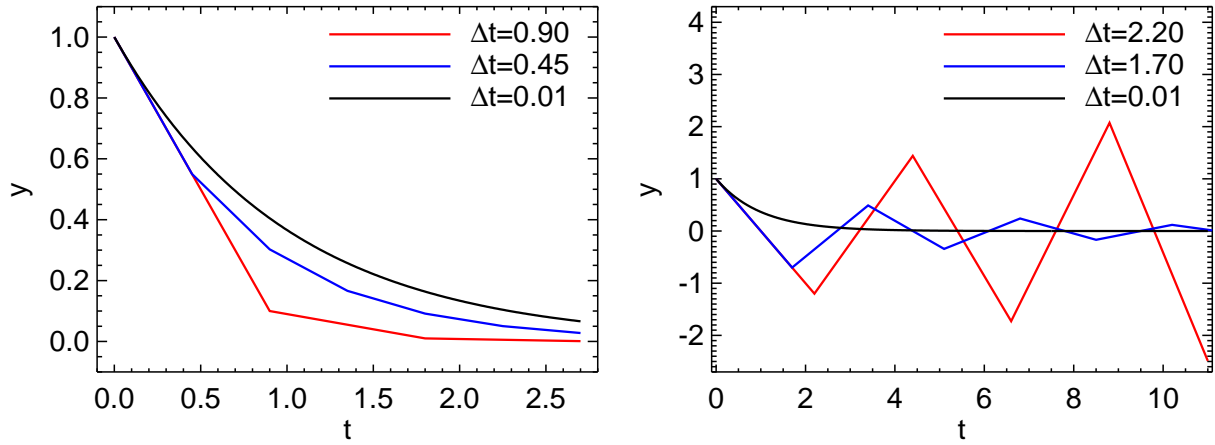


Figure 1: First order integration of ODE with different time-steps.

2.2.3 Simple ODE: remarks

To get accurate results with the Euler scheme (75) the time-step Δt has to be very small. In actual applications one should use a scheme that

- is of **higher order** (e.g. a 4th order Runge-Kutta scheme) to allow much larger time-steps and to improve the efficiency and accuracy of the scheme
- has a build-in **adjustment of the time-step** to guarantee stability even for variable coefficients
- and/or is **specially adapted** for the type of ODE under consideration.

However, the simple scheme in Eq. (75) could – in principle – be used.

2.2.4 Parabolic PDE: heat equation

The **heat equation**

$$\frac{\partial y}{\partial t} = K \frac{\partial^2 y}{\partial x^2} \quad (78)$$

is a simple **parabolic PDE**. With the initial values

$$y(x, t_0) = y_0(x) \quad (79)$$

and boundary values

$$y(x_1, t) = y_1(t) \quad , \quad y(x_2, t) = y_2(t) \quad (80)$$

it models e.g. heat flux or radiative energy transport in the (optically thick) stellar interior. In the following examples the conductivity K is a constant.

2.2.5 Parabolic PDE: discretization

For discrete time-steps on a spatial grid

$$t^n = \Delta t n + t_0 \quad (81)$$

$$x_i = \Delta x i + x_0 \quad (82)$$

the discretization in time and space

$$\frac{\partial y}{\partial t} \rightarrow \frac{y_i^{n+1} - y_i^n}{\Delta t} \quad (83)$$

$$\frac{\partial^2 y}{\partial x^2} \rightarrow \frac{y_{i+1}^n - 2y_i^n + y_{i-1}^n}{\Delta x^2} \quad (84)$$

gives the **explicit Euler scheme**

$$y_i^{n+1} = y_i^n + \frac{\Delta t}{\Delta x^2} K (y_{i+1}^n - 2y_i^n + y_{i-1}^n) . \quad (85)$$

2.2.6 Parabolic PDE: stability

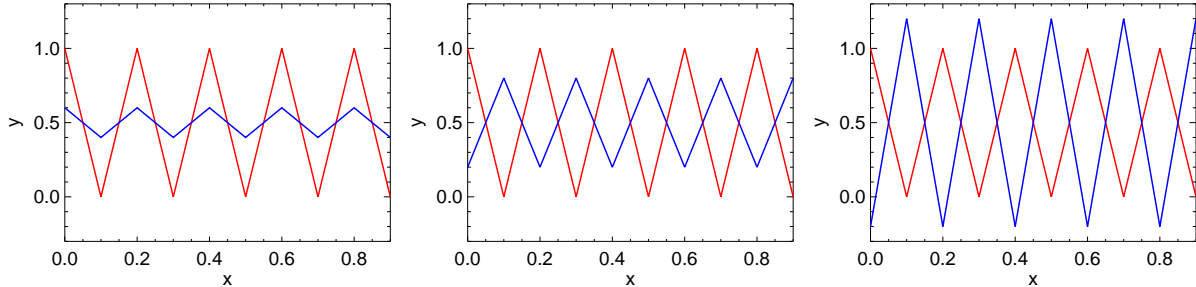


Figure 2: Stability of Euler scheme for heat equation: $\Delta t K / \Delta x^2 = 0.2, 0.4, 0.6$.

Examples for a simple $(1, 0, 1, 0, \dots)$ initial condition (**red**) are displayed in Fig. 2. The

$$\text{criterion for stability:} \quad \Delta t / \Delta x^2 < 1 / (2K) \quad (86)$$

$$\text{criterion for positivity:} \quad \Delta t / \Delta x^2 < 1 / (4K) \quad (87)$$

are comparable to the case of a ODE.

2.2.7 Parabolic PDE: example

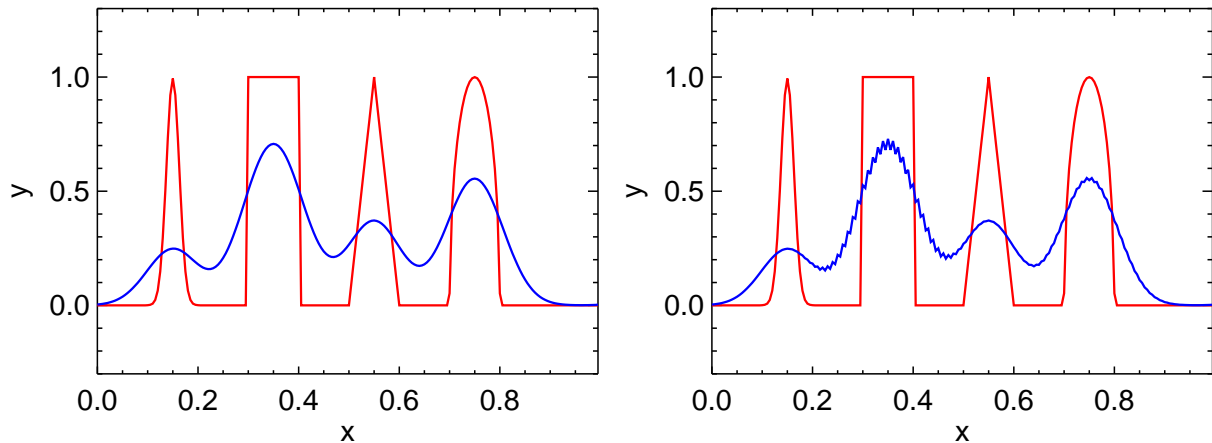


Figure 3: Euler scheme for heat equation.

Examples for “spikes” initial condition (**red**) and periodic boundaries are displayed in Fig. 3 for two time-steps $\Delta t K / \Delta x^2 = 0.1, 0.5$ after 500 or 100 steps, respectively (**blue**).

The slightly too large time-step (0.5) causes the non-decaying spurious oscillations in the right panel.

The simple discretization (85) gives reasonable results.

2.2.8 Linear advection equation: discretization

The prototype of a hyperbolic PDE, the linear advection equation (63), can be discretized for discrete time-steps on a spatial grid

$$t^n = \Delta t n + t_0 \quad (88)$$

$$x_i = \Delta x i + x_0 \quad (89)$$

by replacing

$$\frac{\partial \rho}{\partial t} \rightarrow \frac{\rho_i^{n+1} - \rho_i^n}{\Delta t} \quad (90)$$

$$\frac{\partial \rho}{\partial x} \rightarrow \frac{\rho_{i+1}^n - \rho_{i-1}^n}{2\Delta x} . \quad (91)$$

The result is the **explicit Euler scheme** (“naive” scheme, FTCS scheme)

$$\rho_i^{n+1} = \rho_i^n - \frac{\Delta t}{2\Delta x} v (\rho_{i+1}^n - \rho_{i-1}^n) . \quad (92)$$

This looks quite similar to the discretization of the heat equation (85).

2.2.9 Linear advection equation: crash

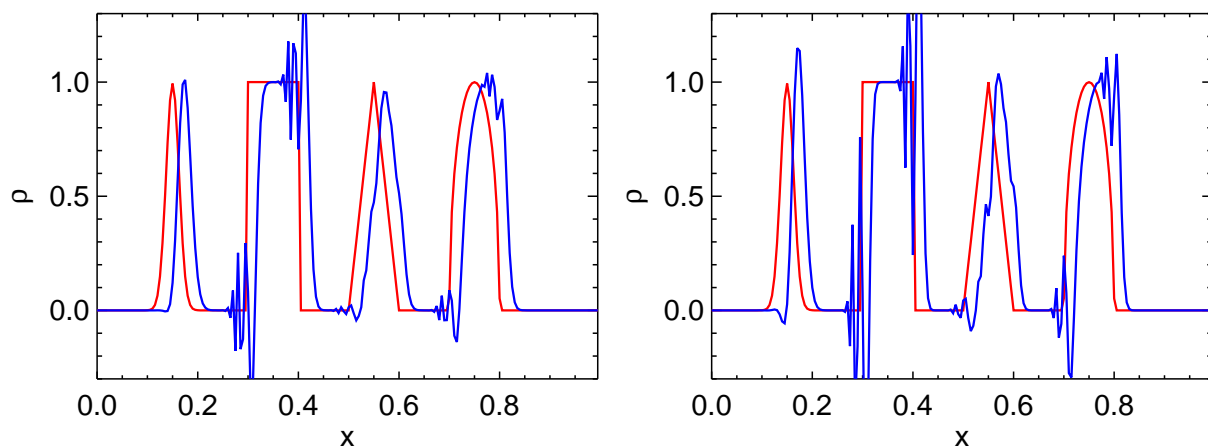


Figure 4: Euler scheme for advection equation.

Examples for “spikes” initial condition (red) and periodic boundaries are displayed in Fig. 4 for two time-steps $\Delta t v / \Delta x = 0.1, 0.5$ after 50 or 10 steps, respectively (blue).

The growing oscillations render the scheme useless.

2.2.10 Linear advection equation: the lesson

Conclusions regarding the naive explicit Euler scheme (92) for the linear advection equation (63) (that worked well for the ODE and the parabolic PDE):

- The scheme is useless.
- Linear stability analysis: The scheme is unconditionally unstable.
- Stability does matter.

Why?

2.3 Basic concepts

2.3.1 Discretization in space: wishlist

- We want: representation of “real” distribution of ρ (\mathbf{v}, e_i) by finite set of numbers
- We need: **restriction**: transformation continuous values \rightarrow discrete representation

- We need: **reconstruction**: transformation discrete representation \rightarrow continuous values
- We get: hints for the discretization of the spatial and temporal operators

Concepts of “restriction” and “reconstruction” are often used during the construction or analysis of a numerical scheme.

These concepts might not show up in the actual algorithm: different concepts may result in the very same scheme.

2.3.2 Discretization in space by finite differences

Finite difference methods:

- Restriction: sampling
- Reconstruction: interpolation (by polynomials)
- Derivatives become finite differences

“Sampling” means: to go from continuous values of $\rho(x)$ to a discrete set of values ρ_i for a grid with $x_i = \Delta x i + x_0$ we set

$$\rho_i = \rho(x_i) . \quad (93)$$

2.3.3 Discretization in space by finite volumes

Finite volume methods:

- Restriction: integration over **control volume**
- Reconstruction: reconstruction (by polynomials)
- Derivatives can become finite differences (or can be avoided)

To go from continuous values of $\rho(x)$ to a discrete set of values ρ_i for a grid with $x_i = \Delta x i + x_0$ we integrate over the “control volume” associated to each grid point. In one dimension that might be

$$\rho_i = \frac{1}{\Delta x} \int_{x_i - \Delta x/2}^{x_i + \Delta x/2} \rho(x) dx . \quad (94)$$

2.3.4 Discretization in space by other methods

Finite element methods:

- Representation by a finite set of simple base functions (piecewise polynomials) with compact (“finite”) support
- Usually used on an unstructured grid to model the flow around complex bodies
- More often used in engineering than in astrophysics

Spectral methods:

- Representation by a finite set of harmonical functions (e.g. sine waves)
- Spatial derivatives become multiplications with wavevector
- Good for flows with small non-linear interactions
- Typically used for flows in the stellar interior (with low Mach numbers)

Smoothed Particle Hydrodynamics (SPH):

- Representation by a finite set of “large particles” that move freely
- Grid is replaced by particle positions
- Particle density translates into fluid density

2.3.5 Discretization in space: grids

In one spatial dimension one can choose between

- **Eulerian grid**: fixed in space
- **Lagrangian grid**: moving with the flow (makes the linear 1D advection trivial)
- Hybrid grid: moving with another speed
- No “grid”: SPH (grid is replaced by particle positions)

In the following examples the grid points will be fixed (Eulerian) and equidistant.

- In multi-dimensions things become more complicated.
- Some advanced “real world” techniques (hierarchical grids perhaps with adaptive mesh refinement) are build upon methods with simple Eulerian grids.

2.3.6 Integral form and weak solution

- Any solution of the advection equation in differential form (63) has to have derivatives.
- However, any function – even a discontinuous one – can be propagated along characteristics (Sect. 2.1.5).

Transformation: linear advection equation in **integral form** (see Fig. 5 and Sect. 1.2.5):

$$\int_{x_0}^{x_1} [\rho(x, t_1) - \rho(x, t_0)] dx + v \int_{t_0}^{t_1} [\rho(x_1, t) - \rho(x_0, t)] dt = 0 \quad (95)$$

Definition: **Weak solution** of PDE in differential form: solution of PDE in integral form.

In smooth regions: weak solution = solution.

2.3.7 Integral form and flux centering

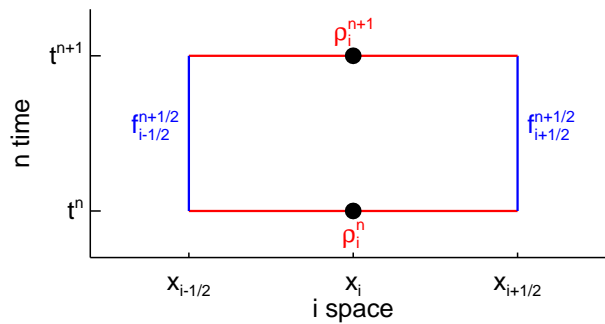


Figure 5: Flux centering.

Integral form from Eq. (95) for one cell and one time-step (see Fig. 5):

$$\underbrace{\int_{x_{i-\frac{1}{2}}}^{x_{i+\frac{1}{2}}} \rho(x, t^{n+1}) dx}_{\Delta x \rho_i^{n+1}} - \underbrace{\int_{x_{i-\frac{1}{2}}}^{x_{i+\frac{1}{2}}} \rho(x, t^n) dx}_{\Delta x \rho_i^n} + \underbrace{\int_{t^n}^{t^{n+1}} v \rho(x_{i+\frac{1}{2}}, t) dt}_{\Delta t f_{i+\frac{1}{2}}^{n+\frac{1}{2}}} - \underbrace{\int_{t^n}^{t^{n+1}} v \rho(x_{i-\frac{1}{2}}, t) dt}_{\Delta t f_{i-\frac{1}{2}}^{n+\frac{1}{2}}} = 0 \quad (96)$$

2.3.8 Centering of quantities, fluxes, and differences

Examples for “natural centering”:

- Quantities at grid points (integer indices): e.g. $\rho_i^n, \rho_{i+1}^n, \dots$
- Spatial differences of quantities (half-integer i indices): e.g. $\Delta\rho_{i+\frac{1}{2}}^n = \rho_{i+1}^n - \rho_i^n$
- Time differences of quantities (half-integer n indices): e.g. $\Delta\rho_i^{n+\frac{1}{2}} = \rho_i^{n+1} - \rho_i^n$
- Fluxes at half-integer i indices (and – in fact – preferably at half-integer n indices) to get update properly centered: $\Delta\rho_i^{n+\frac{1}{2}} = -\frac{\Delta t}{\Delta x} \left(f_{i+\frac{1}{2}}^n - f_{i-\frac{1}{2}}^n \right)$

Effects of “natural centering”:

- $\frac{\rho_{i+1}^n - \rho_i^n}{x_{i+1} - x_i}$ is $O(\Delta x)$ for $\frac{\partial \rho}{\partial x}(x_i)$ and $\frac{\partial \rho}{\partial x}(x_{i+1})$.
- $\frac{\rho_{i+1}^n - \rho_i^n}{x_{i+1} - x_i}$ is $O(\Delta x^2)$ for $\frac{\partial \rho}{\partial x}(x_{i+\frac{1}{2}})$.
- $\frac{\rho_{i+1}^n - \rho_{i-1}^n}{x_{i+1} - x_{i-1}}$ is $O(\Delta x^2)$ for $\frac{\partial \rho}{\partial x}(x_i)$.

2.3.9 Update formula in conservation form

After computing e.g. from the fluxes in the cells

$$f(\rho_i^n) = v \rho_i^n \quad (97)$$

the fluxes at cell boundaries

$$f_{i+\frac{1}{2}}^n \quad (98)$$

that characterize a method, the update can be done by the formula

$$\rho_i^{n+1} = \rho_i^n - \frac{\Delta t}{\Delta x} \left(f_{i+\frac{1}{2}}^n - f_{i-\frac{1}{2}}^n \right) . \quad (99)$$

This is the **conservation form** because the density changes only due to fluxes through the boundaries and is conserved otherwise,

$$\sum_{i=i_0}^{i_1} \rho_i^{n+1} = \sum_{i=i_0}^{i_1} \rho_i^n + \frac{\Delta t}{\Delta x} \sum_{i=i_0}^{i_1} \left(f_{i+\frac{1}{2}}^n - f_{i-\frac{1}{2}}^n \right) \quad (100)$$

$$= \sum_{i=i_0}^{i_1} \rho_i^n + \frac{\Delta t}{\Delta x} \left[f_{i_1+\frac{1}{2}}^n + \sum_{i=i_0}^{i_1-1} \left(f_{i+\frac{1}{2}}^n - f_{i+\frac{1}{2}}^n \right) - f_{i_0-\frac{1}{2}}^n \right] \quad (101)$$

$$= \sum_{i=i_0}^{i_1} \rho_i^n + \frac{\Delta t}{\Delta x} \left(f_{i_1+\frac{1}{2}}^n - f_{i_0-\frac{1}{2}}^n \right) . \quad (102)$$

2.3.10 Stencil diagrams

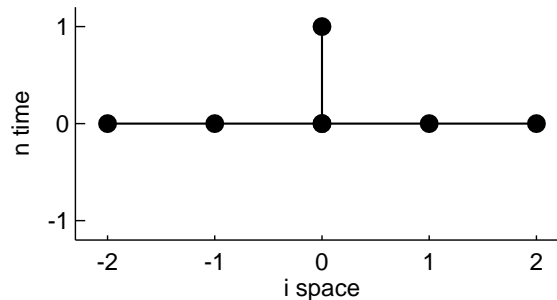


Figure 6: Stencil diagram.

The density ρ_i^{n+1} at grid point i and time-step $n + 1$ depends on values at the old time-step n (direct **numerical domain of dependence**, **stencil**)

$$\rho_{i-k}^n, \rho_{i-k+1}^n, \dots, \rho_{i+l}^n \quad (103)$$

This is sketched in a so-called **stencil diagram** as in Fig. 6.

Looking the other way, a stencil diagram tells also which points

$$\rho_{i-l}^{n+1}, \rho_{i-l+1}^{n+1}, \dots, \rho_{i+k}^{n+1} \quad (104)$$

at the new time-step $n + 1$ are influenced by ρ_i^n (**range of influence**).

2.3.11 Stencil diagrams: spatial centering

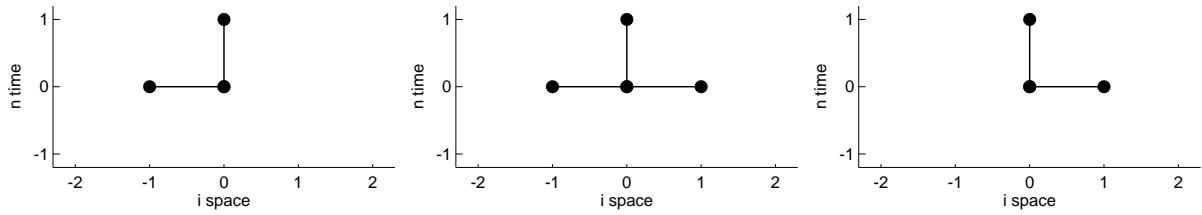


Figure 7: Stencil diagrams with different spatial centering: FTBS, FTCS, FTFS.

Figure 7 shows stencil diagrams for 3 schemes with FT (forward-time) centering and different spatial centerings:

- **BS**: backward-space
- **CS**: center-space
- **FS**: forward-space

The middle panel corresponds to the FTCS scheme from Eq. (92).

2.3.12 Stencil diagrams: centering in time

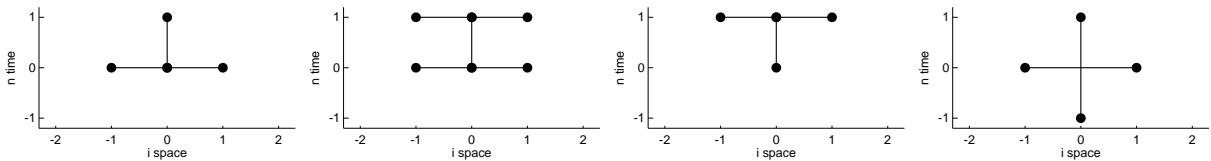


Figure 8: Stencil diagrams with different time-centering: FTCS, time-centered implicit, BTCS, CTCS (leapfrog).

Figure 8 shows stencil diagrams for 4 schemes with CS and different time centering:

- **FT**: forward-time (explicit)
- **time-centered implicit**: (implicit)
- **BT**: backward-time (fully implicit)
- **CT, Leapfrog**: center-time (explicit, uses 3 time planes)

In implicit schemes each value at the new time level typically depends on all values at the old level: The full domain of dependence is larger than the direct domain of dependence.

2.3.13 CFL condition

Due to the finite travelling speed of waves hyperbolic PDEs have a finite **physical domain of dependence**.

Courant-Friedrichs-Levy condition (**CFL condition**):

- **The full numerical domain of dependence must contain the physical domain of dependence.**

The CFL condition is necessary for stability (but not sufficient).

2.3.14 Truncation error

A sufficiently smooth function can be expanded in a Taylor series:

$$\rho(x + \Delta x, t) = \sum_{l=0}^{\infty} \frac{1}{l!} \left. \frac{\partial^l \rho}{\partial x^l} \right|_{x,t} \Delta x^l = \rho(x, t) + \left. \frac{\partial \rho}{\partial x} \right|_{x,t} \Delta x + O(\Delta x^2) . \quad (105)$$

Solving for $\frac{\partial \rho}{\partial x}$ gives

$$\frac{\partial \rho}{\partial x} = \frac{\rho(x + \Delta x, t) - \rho(x, t)}{\Delta x} + O(\Delta x) . \quad (106)$$

Repeating this for the time derivative and applying it to an entire PDE (FTFS) gives

$$\underbrace{\frac{\partial \rho}{\partial t} + v \frac{\partial \rho}{\partial x}}_{\text{PDE}} = \underbrace{\frac{\rho_i^{n+1} - \rho_i^n}{\Delta t} + v \frac{\rho_{i+1}^n - \rho_i^n}{\Delta x}}_{\text{numerical scheme}} + \underbrace{O(\Delta t, \Delta x)}_{\text{truncation error}} . \quad (107)$$

The **order** of the **truncation error** is $O(\Delta t, \Delta x)$ in this case (FTFS).

A high order of the truncation error (both in Δt and Δx) hints at **good accuracy for smooth functions**.

2.3.15 Consistency – stability – convergence

- **Consistency:** A numerical scheme is **consistent** if its discrete operator (with finite differences) converges towards the continuous operator (with derivatives) of the PDE for $\Delta t, \Delta x \rightarrow 0$ (vanishing truncation error).
- **Stability:** “Noise” (from initial conditions, round-off errors, ...) does not grow.
- **Convergence:** The solution of the numerical scheme converges towards the real solution of the PDE for $\Delta t, \Delta x \rightarrow 0$.

Lax’s equivalence theorem: “Given a properly posed initial value problem and a finite-difference approximation to it that satisfies the consistency condition, stability is the necessary and sufficient condition for convergence.”

- **Consistency:** discrete operator $\xrightarrow{\Delta t, \Delta x \rightarrow 0}$ PDE operator
- **Stability:** discrete operator does not amplify “noise”
- **Convergence:** Numerical solution $\xrightarrow{\Delta t, \Delta x \rightarrow 0}$ real solution

Lax’s equivalence theorem: **consistency + stability \Leftrightarrow convergence**

2.3.16 Derivations of donor cell scheme

Donor cell scheme (FTBS, stencil in Sect. 2.3.11, example later in Sect. 2.4.5):

$$\rho_i^{n+1} = \rho_i^n - \frac{\Delta t v}{\Delta x} (\rho_i^n - \rho_{i-1}^n) . \quad (108)$$

1. Discrete differences:

- Characteristic curves: mass flows from left to right
- Replacement: CS of naive scheme \rightarrow difference in **upwind** direction: BS

2. Characteristics + interpolation:

- Follow characteristic curve from ρ_i^{n+1} back in time
- Interpolate between ρ_{i-1}^n and ρ_i^n (linearly)

3. Reconstruct–Solve–Average (RSA, Godunov-type method):

- Finite volumes (reconstruction-evolution, Reconstruct-Propagate-Average)
- Reconstruct run of ρ within each cell (here: assume constant ρ)
- Use exact continuous solution for the time evolution
- Average intermediate continuous result to get single value in each cell

2.3.17 Further concepts

Important properties of a numerical scheme:

- **Consistency** (otherwise it does not describe the PDE)
- **Stability** (and therefore **convergence** of the solution)
- **Conservativity** (to prevent leakages)

Further desirable properties of a numerical scheme or code:

- **Accuracy**: high-order convergence in smooth regions (high-order truncation error), good approximation even at finite resolution, minimal artifacts near discontinuities
- **Positivity** (boundedness): ρ, P, T always positive
- **Simplicity**: code should be easy to understand, maintain, and extend
- **Efficiency**: code should be fast (on a variety of machines)

The non-linear system of the hydrodynamic equations will put additional weight on conservativity and positivity.

2.4 Examples

2.4.1 Parameter of the following examples

Boundary conditions influence the properties of real world hydrodynamic flows.

Linear 1D advection: infinite domain without boundaries.

Actual implementation of boundary conditions in numerical experiments:

- Adding and filling **ghost cells**
- Number of ghost cells: depends on stencil
- In examples: **periodic boundary conditions**

Grid settings:

$$i_{\text{total}} = 200 , \quad n_{\text{total}} = 500 , \quad \frac{\Delta t v}{\Delta x} = 0.4 \Rightarrow \text{one revolution} \quad (109)$$

Initial condition: “spikes” (Gaussian, rectangle, triangle, half-ellipse), see Jiang & Shu (1996).

2.4.2 Naive FTCS scheme

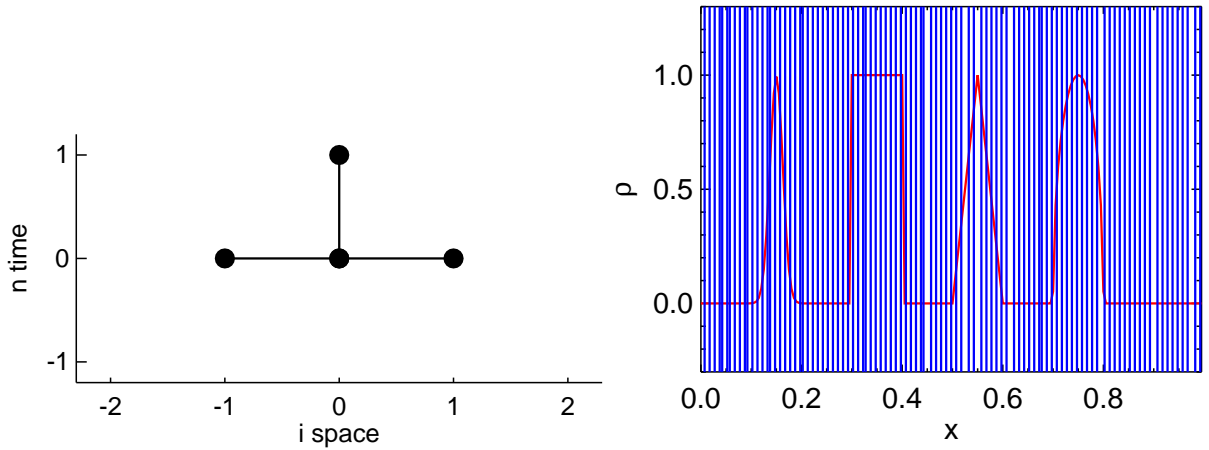


Figure 9: Naive scheme: stencil diagram and (disastrous) test result.

Figure 9: **naive scheme** (Euler scheme, FTCS, Sect. 2.2.9) from Eq. (92) with flux at $i + \frac{1}{2}$

$$f_{i+\frac{1}{2}}^n = \frac{1}{2} [f(\rho_{i+1}^n) + f(\rho_i^n)] . \quad (110)$$

The oscillations already seen in Fig. 4 grow exponentially. After some time the numerical result does not have the faintest resemblance to true solution.

2.4.3 Implicit centered scheme

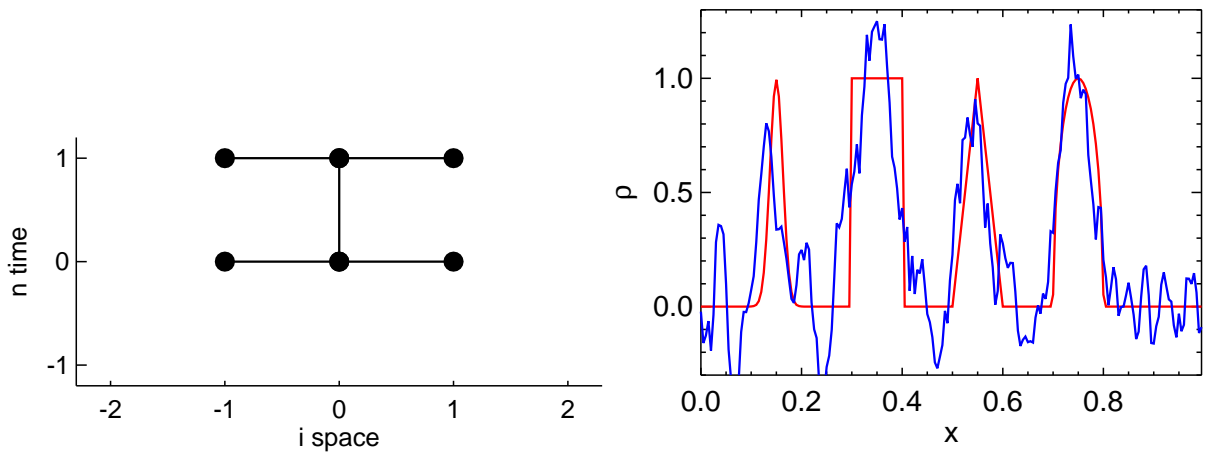


Figure 10: Implicit centered scheme: stencil diagram and test result.

Figure 10: **Implicit centered scheme** with flux

$$f_{i+\frac{1}{2}}^n = \frac{1}{4} [f(\rho_{i+1}^n) + f(\rho_i^n)] + \frac{1}{4} [f(\rho_{i+1}^{n+1}) + f(\rho_i^{n+1})] . \quad (111)$$

The centering of the scheme in space and time seemed promising. However, the initial condition is severely distorted.

2.4.4 BTCS scheme

Figure 11: fully implicit **BTCS scheme** with flux

$$f_{i+\frac{1}{2}}^n = \frac{1}{2} [f(\rho_{i+1}^{n+1}) + f(\rho_i^{n+1})] . \quad (112)$$

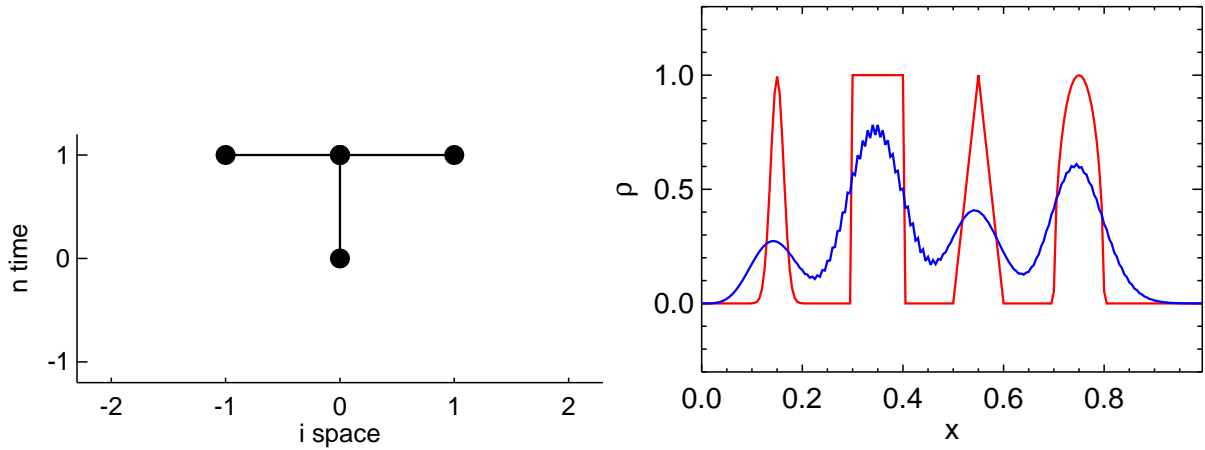


Figure 11: BTCS scheme: stencil diagram and test result.

The fully implicit treatment takes effect: the result looks almost smooth (with some non-decaying small-scale wiggles) but is smeared out heavily.

2.4.5 Donor cell (FTBS) scheme

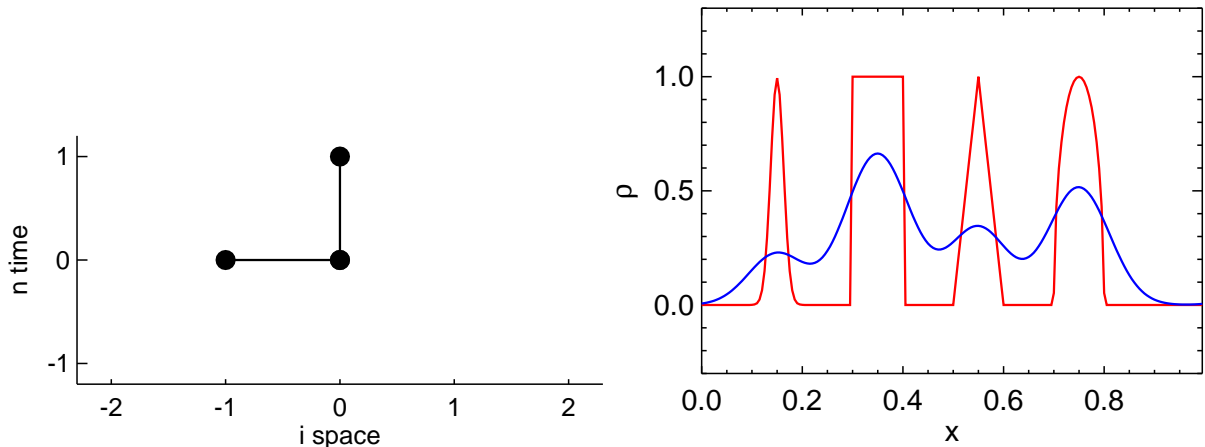


Figure 12: Stencil and example for donor cell scheme.

Figure 12: **donor cell scheme** (FTBS, 1st order upwind method, derived in Sect. 2.3.16), with flux

$$f_{i+\frac{1}{2}}^n = f(\rho_i^n) \quad . \quad (113)$$

The result is wonderfully smooth but smeared out severely. Upwinding seems promising to achieve stability. However, the accuracy of the scheme has to be improved.

2.4.6 FTFS scheme

Figure 13: **FTFS scheme** with flux

$$f_{i+\frac{1}{2}}^n = f(\rho_{i+1}^n) \quad . \quad (114)$$

Small-scale oscillations grow even faster than for the naive scheme and render the FTFS scheme useless (at least for $v > 0$), too.

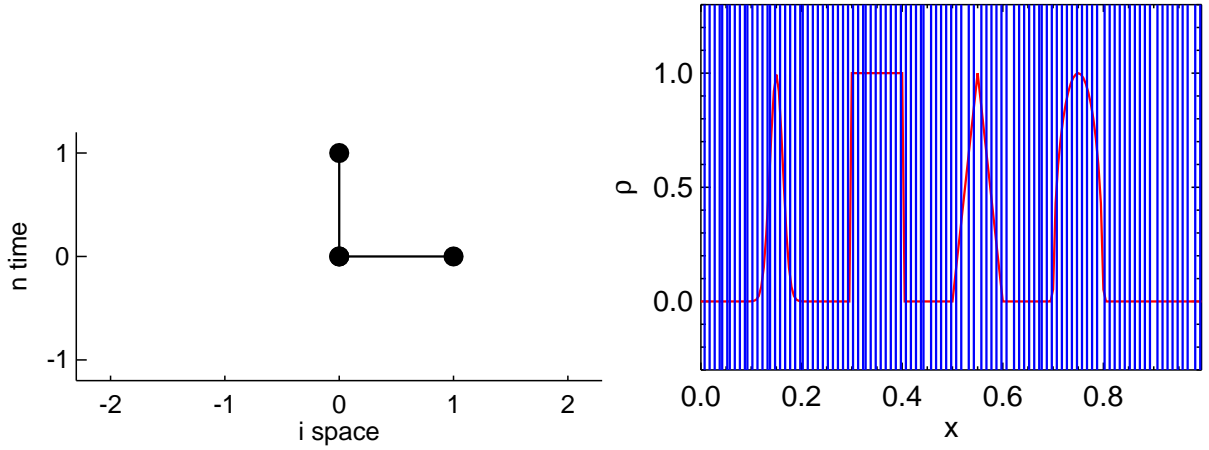


Figure 13: FTFS scheme: stencil diagram and (disastrous) test result.

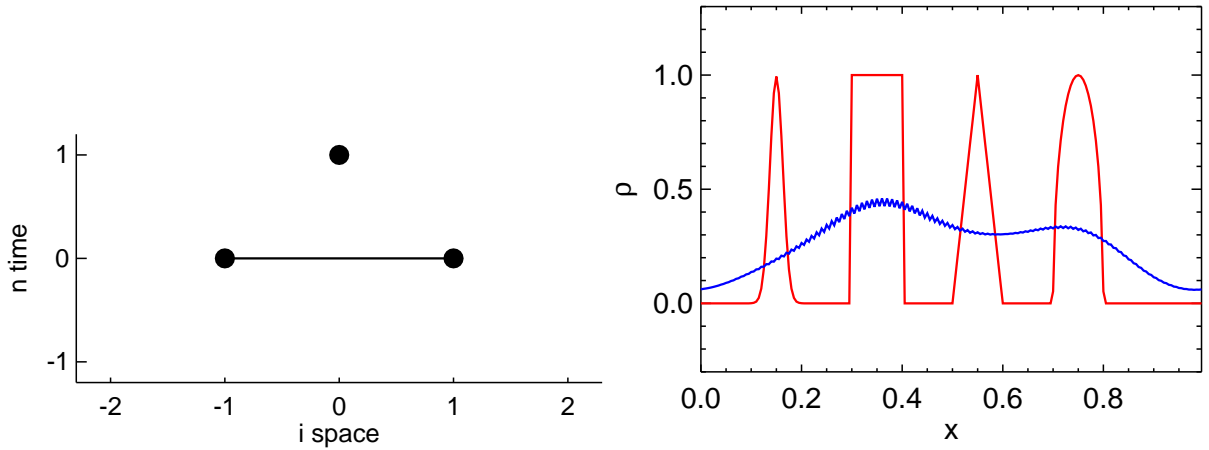


Figure 14: Stencil and example for Lax-Friedrichs scheme.

2.4.7 Lax-Friedrichs scheme

Figure 14: **Lax-Friedrichs scheme** with flux

$$f_{i+\frac{1}{2}}^n = \frac{1}{2} [f(\rho_{i+1}^n) + f(\rho_i^n)] - \frac{1}{2} \frac{\Delta x}{\Delta t} [\rho_{i+1}^n - \rho_i^n] . \quad (115)$$

The smearing is so strong that not even the number of the initial spikes is conserved. And there are some non-decaying small-scale wiggles left.

Note: odd-even decoupling.

2.4.8 Lax-Wendroff scheme

Figure 15: **Lax-Wendroff scheme** is $O(\Delta x^2, \Delta t^2)$ with flux

$$f_{i+\frac{1}{2}}^n = \frac{1}{2} [f(\rho_{i+1}^n) + f(\rho_i^n)] - \frac{1}{2} \frac{v^2 \Delta t}{\Delta x} [\rho_{i+1}^n - \rho_i^n] . \quad (116)$$

The result is smooth with considerable overshoot (that does not much grow with time anymore). This second order scheme might be useful for more regular initial conditions.

2.4.9 Beam-Warming scheme

Figure 16: **Beam-Warming scheme** is $O(\Delta x^2, \Delta t^2)$ with flux

$$f_{i+\frac{1}{2}}^n = \frac{1}{2} [3f(\rho_i^n) - f(\rho_{i-1}^n)] - \frac{1}{2} \frac{v^2 \Delta t}{\Delta x} [\rho_i^n - \rho_{i-1}^n] . \quad (117)$$

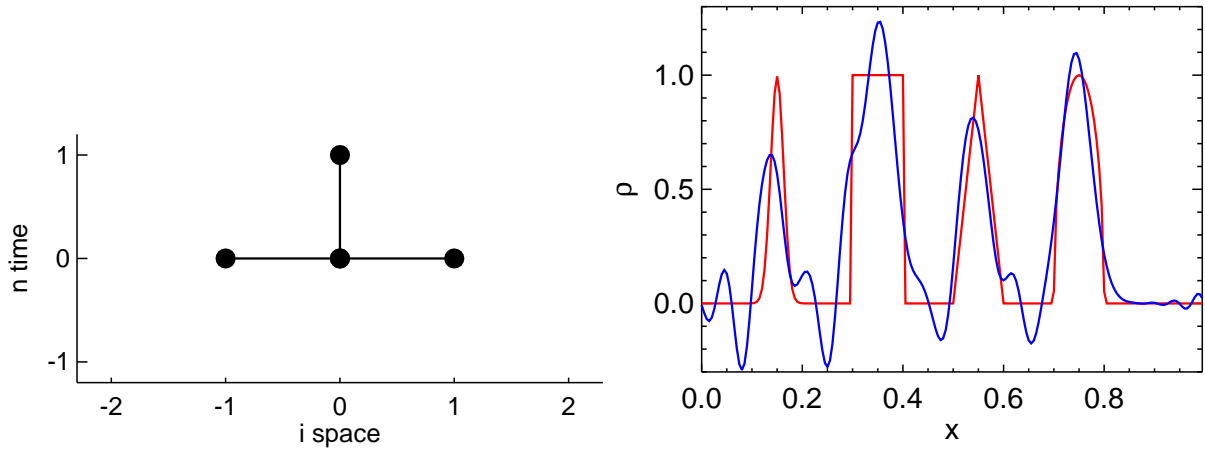


Figure 15: Stencil and example for Lax-Wendroff scheme.

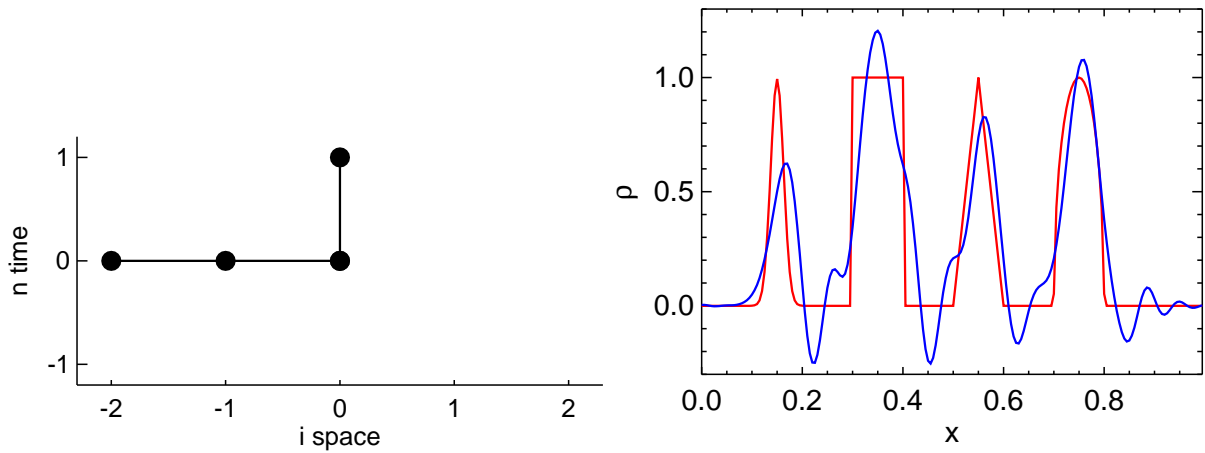


Figure 16: Stencil and example for Beam-Warming scheme.

The result is smooth with considerable overshoot (that does not much grow with time anymore). This second order scheme might be useful for more regular initial conditions.

2.4.10 Fromm scheme

Figure 17: **Fromm scheme** is $O(\Delta x^2, \Delta t^2)$ with flux

$$f_{i+\frac{1}{2}}^n = \frac{1}{2} \left(f_{\text{Lax-Wendroff}, i+\frac{1}{2}}^n + f_{\text{Beam-Warming}, i+\frac{1}{2}}^n \right). \quad (118)$$

The result is smooth with some amount of overshoot. The initial shape of the spikes is recognizable. So far the best scheme, if the overshoot can be accepted.

See Sect. 2.6.6.

2.5 Analysis of schemes

2.5.1 Overshoot

Figure 18 shows the standard example after only $n=20$ time-steps for the Lax-Wendroff (Sect. 2.4.8) and the Beam-Warming scheme (Sect. 2.4.9) displaying overshooting post- and pre-shock oscillations.

This **Gibb's phenomenon** is closely related to overshoot of parabolic (or higher-order) interpolation schemes.

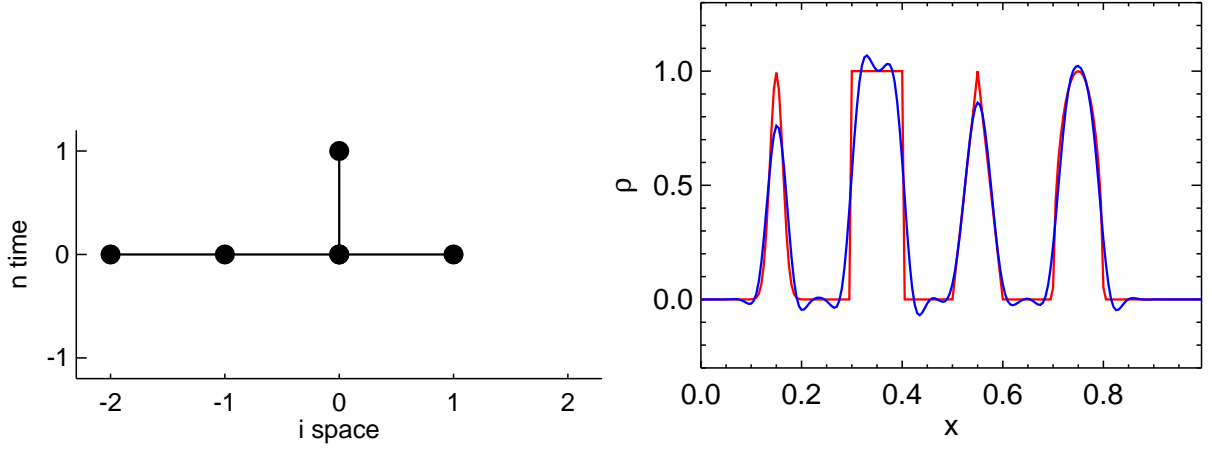


Figure 17: Stencil and example for Fromm scheme.

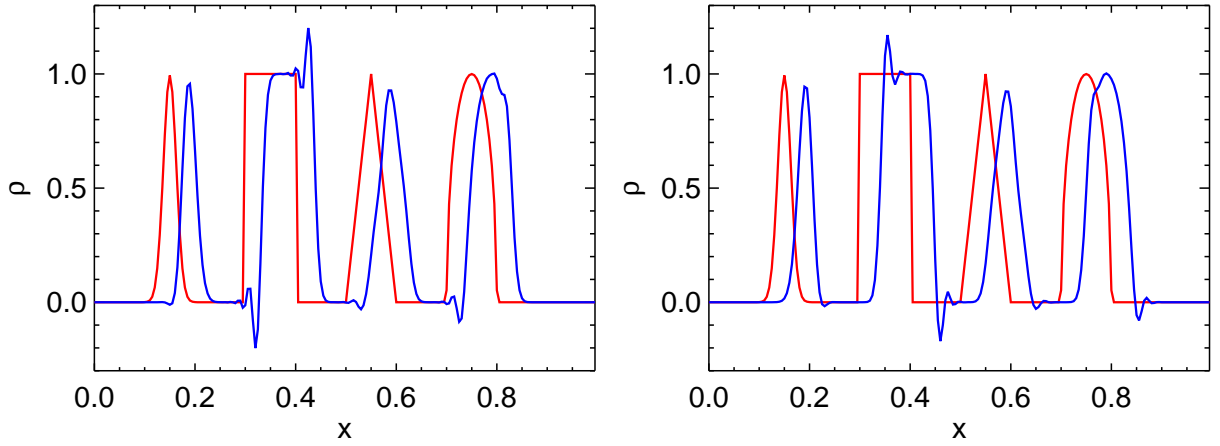


Figure 18: Lax-Wendroff and Beam-Warming scheme.

2.5.2 Artificial viscosity

Inserting the Lax-Friedrichs flux (115) into the conservative update formula (99) results in

$$\rho_i^{n+1} = \underbrace{\rho_i^n - \frac{\Delta t}{2\Delta x} [v\rho_{i+1}^n - v\rho_{i-1}^n]}_{\text{FTCS scheme}} + \underbrace{\frac{1}{2} [\rho_{i+1}^n - 2\rho_i^n + \rho_{i-1}^n]}_{\text{artificial viscosity}}. \quad (119)$$

The last term looks like a 2nd derivative and is called **artificial viscosity**. In general, the flux of any scheme can be written in the form

$$f = \underbrace{f_{\text{FTCS}}}_{\text{FTCS flux}} + \underbrace{(f - f_{\text{FTCS}})}_{\text{flux due to artificial viscosity}}. \quad (120)$$

Sometimes, the Lax-Wendroff flux is used as reference,

$$f = \underbrace{f_{\text{Lax-Wendroff}}}_{\text{Lax-Wendroff flux}} + \underbrace{(f - f_{\text{Lax-Wendroff}})}_{\text{flux due to artificial viscosity}}. \quad (121)$$

2.5.3 Modified equation for the FTFS scheme I

Keeping one more term in Eq. (105) we get instead of Eq. (107) the equation

$$\underbrace{\frac{\partial \rho}{\partial t} + v \frac{\partial \rho}{\partial x}}_{\text{PDE}} + \underbrace{\frac{1}{2} \frac{\partial^2 \rho}{\partial t^2} \Delta t + \frac{1}{2} v \frac{\partial^2 \rho}{\partial x^2} \Delta x}_{\text{2nd order terms}} = \underbrace{\frac{\rho_i^{n+1} - \rho_i^n}{\Delta t} + v \frac{\rho_{i+1}^n - \rho_i^n}{\Delta x}}_{\text{numerical scheme}} + \underbrace{O(\Delta t^2, \Delta x^2)}_{\text{rest error}} . \quad (122)$$

modified equation

Now, the error is $O(\Delta t^2, \Delta x^2)$ instead of $O(\Delta t, \Delta x)$.

I.e., the numerical scheme describes the **modified equation**

$$\frac{\partial \rho}{\partial t} + v \frac{\partial \rho}{\partial x} + \frac{1}{2} \frac{\partial^2 \rho}{\partial t^2} \Delta t + \frac{1}{2} v \frac{\partial^2 \rho}{\partial x^2} \Delta x = 0 \quad (123)$$

better than the original PDE.

2.5.4 Modified equation for the FTFS scheme II

To replace $\frac{\partial^2 \rho}{\partial t^2}$ in the modified equation (123) we write

$$\frac{\partial^2 \rho}{\partial t^2} \Delta t + v \frac{\partial^2 \rho}{\partial x^2} \Delta x = \frac{\partial}{\partial t} \left(-v \frac{\partial \rho}{\partial x} \right) \Delta t + v \frac{\partial^2 \rho}{\partial x^2} \Delta x + O(\Delta t^2, \Delta x^2) \quad (124)$$

$$= -v \frac{\partial}{\partial x} \left(\frac{\partial \rho}{\partial t} \right) \Delta t + v \frac{\partial^2 \rho}{\partial x^2} \Delta x + O(\Delta t^2, \Delta x^2) \quad (125)$$

$$= v^2 \frac{\partial^2 \rho}{\partial x^2} \Delta t + v \frac{\partial^2 \rho}{\partial x^2} \Delta x + O(\Delta t^2, \Delta x^2) \quad (126)$$

$$= v \Delta x \left(\frac{v \Delta t}{\Delta x} + 1 \right) \frac{\partial^2 \rho}{\partial x^2} + O(\Delta t^2, \Delta x^2) \quad (127)$$

and get for the **modified equation** for the FTFS scheme

$$\frac{\partial \rho}{\partial t} + v \frac{\partial \rho}{\partial x} + \frac{1}{2} v \Delta x \left(\frac{v \Delta t}{\Delta x} + 1 \right) \frac{\partial^2 \rho}{\partial x^2} = 0 . \quad (128)$$

The coefficient of the additional diffusion term is positive: it describes **anti-diffusion**.

2.5.5 Modified equation for the FTBS scheme

A similar procedure gives the modified equation for the FTBS scheme

$$\frac{\partial \rho}{\partial t} + v \frac{\partial \rho}{\partial x} - \frac{1}{2} v \Delta x \left(1 - \frac{v \Delta t}{\Delta x} \right) \frac{\partial^2 \rho}{\partial x^2} = 0 . \quad (129)$$

The coefficient of the additional diffusion term is negative if the CFL condition is fulfilled:

It describes **diffusion**, clearly seen in Fig. 12 (compare the example for the heat equation in Fig. 3).

2.5.6 Linear stability analysis of original PDE

Lets see what happens to waves in the linear advection equation (63). For the ansatz

$$\rho(x, t) = A(t) e^{-jkx} \quad (130)$$

with $j^2 = -1$ we get

$$\frac{dA}{dt} + v(-jk)A = 0 \Rightarrow \frac{dA}{dt} = jvkA \Rightarrow A = A_0 e^{jvkt} , \quad (131)$$

$$\rho = A_0 e^{j(\omega t - kx)} \quad (132)$$

with

$$\text{abs}(A) = \text{abs}(A_0) = \text{const} \quad , \quad (133)$$

$$\omega = vk \quad . \quad (134)$$

Dispersion relation (134): no dispersion, all waves move with the same speed v .

Eq. (133): amplitude remains constant – without any diffusion.

2.5.7 Linear stability analysis: use

Linear stability analysis tells about stability – of linear schemes for linear equations.

Linear stability \Rightarrow convergence for consistent schemes (Sect. 2.3.15).

Ansatz: for

$$\rho_i^n = e^{-jik\Delta x} \quad (135)$$

with $k \leq k_0 = \frac{\pi}{\Delta x}$ we search $A \in \mathbb{C}$ with

$$\rho_i^{n+1} = A \rho_i^n = A e^{-jik\Delta x} \quad . \quad (136)$$

Amount $\text{abs}(A)$ of $A \Rightarrow$ damping (diffusion) or growth (instability) of waves.

Phase of $A \Rightarrow$ wave speed and dispersion.

Ideally $A = e^{j\omega\Delta t}$ with $\omega = vk$.

2.5.8 Linear stability analysis of naive FTCS scheme

Applying ansatz (135) to the naive FTCS scheme Eq. (92) gives

$$A e^{-jik\Delta x} = e^{-jik\Delta x} - \frac{\Delta t}{\Delta x} v \frac{1}{2} \left(e^{-j(i+1)k\Delta x} - e^{-j(i-1)k\Delta x} \right) \quad . \quad (137)$$

Multiplying with $e^{jik\Delta x}$ and using the **Courant number**

$$\alpha := \frac{\Delta t}{\Delta x} v \quad (138)$$

we get

$$A = 1 - \alpha \frac{1}{2} \left(e^{-jk\Delta x} - e^{jk\Delta x} \right) = 1 + j\alpha \sin k\Delta x \quad , \quad (139)$$

$$\text{abs}(A) = \left(1 + \alpha^2 \sin^2 k\Delta x \right)^{\frac{1}{2}} \quad , \quad (140)$$

$$\text{abs}(A) > 1 \quad \text{for } 0 < k\Delta x < \pi \quad , \quad \alpha > 0 \quad . \quad (141)$$

All waves except the ones with smallest wavenumber grow exponentially in time:

The scheme is **unconditionally unstable**, independent of the time-step.

2.5.9 Linear stability analysis of donor cell (FTBS) scheme

Applying ansatz (135) to the donor cell scheme Eq. (108) gives, using Eq. (138),

$$A = 1 - \alpha \left(1 - e^{jk\Delta x} \right) = 1 - \alpha (1 - \cos k\Delta x) + j\alpha \sin k\Delta x \quad , \quad (142)$$

$$\text{abs}(A) = \left[1 - 2 \underbrace{(\alpha - \alpha^2)}_{\geq 0 \text{ for } \alpha \in [0,1]} \underbrace{(1 - \cos k\Delta x)}_{\geq 0} \right]^{\frac{1}{2}} \quad , \quad (143)$$

$$\text{abs}(A) \leq 1 \quad \text{for } \alpha \in [0, 1] \quad . \quad (144)$$

The donor cell scheme is **stable** if the **CFL condition** is fulfilled,

$$\frac{\Delta t}{\Delta x} v \in [0, 1] \quad . \quad (145)$$

Note: $v \geq 0$ is required (for $v \leq 0$ use FTFS).

Note: $\text{abs}(A) < 1$ is possible: **numerical viscosity**

Note: phase(A) $\neq vk\Delta t$: **dispersion**

2.5.10 Linear stability analysis: remarks

Further issues:

- Severe restriction: linear PDE and linear scheme
- Growth of amplitude means instability – and stability otherwise
- Correct solution (constant amplitude) right at the border to instability
- Decline of amplitude indicates numerical viscosity
- Constant amplitude achievable by time-symmetric schemes (but: wiggles, dispersion)

Conclusions:

- No linear scheme is really satisfying.

2.6 Non-linear schemes

2.6.1 Godunov's idea

Discretization paradigms (see Sect. 2.3.16):

- Finite differences: replace derivatives by differences
- Characteristics: follow characteristics back in time and interpolate at old time-level
- Reconstruct-Solve-Average (RSA): Godunov-type finite-volume scheme

RSA: three steps:

- **Reconstruct** $\rho(x)$ from ρ_i .
- **Solve** the exact problem for Δt : shift reconstructed function.
- **Average** $\rho(x)$ in each cell to get ρ_i .

Note: Exact solution (and reconstruction) can handle shocks \Rightarrow numerical scheme can handle shocks.

2.6.2 Monotonicity

Transport and averaging are easy and well determined. The entire algorithm is determined by the **reconstruction** scheme.

- Consistency: “reasonable” interpolation
- Accuracy: high-order polynomials
- Conservativity: proper flux formulation
- Stability, positivity: **monotonicity** preservation

Definition: **Total variation**:

$$TV = \sum_i \text{abs}(\rho_{i+1} - \rho_i) \quad (146)$$

TVD property: A scheme has the TVD property (is “Total Variation Diminishing”) if TV does not increase in time.

\Rightarrow Non-linear stability criterion.

Godunov's theorem: linear monotonicity-preserving methods are first-order accurate, at best.

\Rightarrow Try a non-linear scheme.

2.6.3 Flux of PLM schemes

- Donor cell scheme: constant ρ within each cell
- Improvement: **piecewise linear method (PLM)**: reconstruction by linear function in each cell

Once we know the cell average ρ_i and the slope $\delta\rho_i$, we get the flux over Δt from

$$f_{i\pm\frac{1}{2}} = v \left\{ \rho_i + \frac{1}{2} \delta\rho_i \operatorname{sign}(v) \left[1 - \operatorname{abs}(v) \frac{\Delta t}{\Delta x} \right] \right\} . \quad (147)$$

If the boundary value in the cell is used for the entire cell we get

$$f_{i\pm\frac{1}{2}} = v \left\{ \rho_i + \frac{1}{2} \delta\rho_i \operatorname{sign}(v) \right\} . \quad (148)$$

For $v > 0$ we get from each cell ρ_i the flux $f_{i+\frac{1}{2}}$.

For $v < 0$ we get from each cell ρ_i the flux $f_{i-\frac{1}{2}}$.

2.6.4 Examples: PLM: slopes with linear parameter dependence

Slopes of already encountered (linear) schemes:

Donor cell scheme (slope zero):

$$\delta\rho_i = 0 \quad (149)$$

Lax-Wendroff scheme:

$$\delta\rho_i = \rho_{i+1} - \rho_i \quad (150)$$

Beam-Warming scheme:

$$\delta\rho_i = \rho_i - \rho_{i-1} \quad (151)$$

Fromm scheme:

$$\delta\rho_i = \frac{1}{2} (\rho_{i+1} - \rho_{i-1}) \quad (152)$$

2.6.5 PLM: slope-limiter

A slope can be written as

$$\delta\rho_i = \Phi \left(\frac{\rho_i - \rho_{i-1}}{\rho_{i+1} - \rho_i} \right) \delta\rho_i(\text{Lax-Wendroff}) \quad (153)$$

with the help of a (possibly non-linear) **slope-limiter** or **flux-limiter**

$$\Phi \left(\frac{\rho_i - \rho_{i-1}}{\rho_{i+1} - \rho_i} \right) = \frac{\delta\rho_i}{\delta\rho_i(\text{Lax-Wendroff})} \quad (154)$$

A related concept is **flux-averaging**.

Note: The slope-limiter for the Lax-Wendroff scheme is 1.

Note: The slope-limiter for the donor cell scheme is 0.

2.6.6 PLM scheme with Minmod slope-limiter

Figure 19: **PLM scheme** with **Minmod slope** (minimum allowed 2nd order slope),

$$\begin{aligned} \delta\rho_i = & \min(\max(\rho_i - \rho_{i-1}, 0), \max(\rho_{i+1} - \rho_i, 0)) + \\ & \max(\min(\rho_i - \rho_{i-1}, 0), \min(\rho_{i+1} - \rho_i, 0)) . \end{aligned} \quad (155)$$

See Sect. 2.4.10.

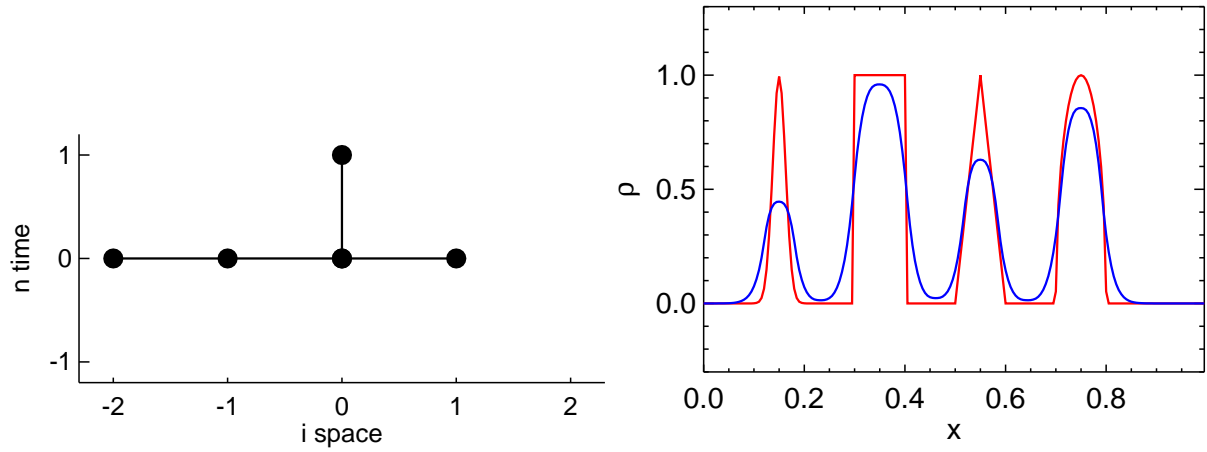


Figure 19: Stencil and example for PLM scheme with Minmod slope-limiter.

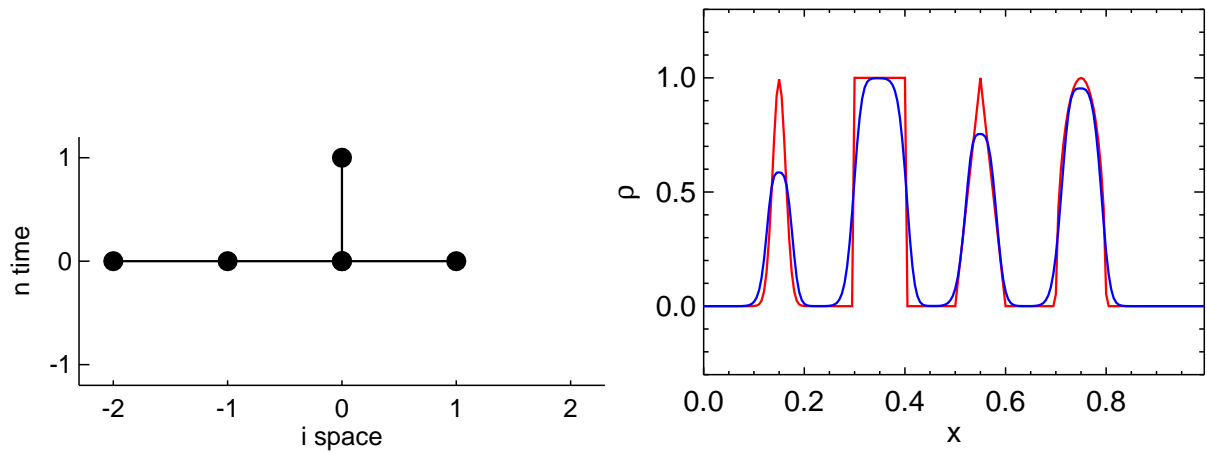


Figure 20: Stencil and example for PLM scheme with vanLeer slope-limiter.

2.6.7 PLM scheme with vanLeer slope-limiter

Figure 20: **PLM scheme** with **vanLeer slope** (harmonic mean of slopes),

$$\delta\rho_i = \begin{cases} \frac{1}{\frac{1}{2}\left(\frac{1}{\rho_i - \rho_{i-1}} + \frac{1}{\rho_{i+1} - \rho_i}\right)} & \text{if } (\rho_i - \rho_{i-1})(\rho_{i+1} - \rho_i) > 0 \\ 0 & \text{elsewhere} \end{cases} . \quad (156)$$

2.6.8 PLM scheme with Superbee slope-limiter

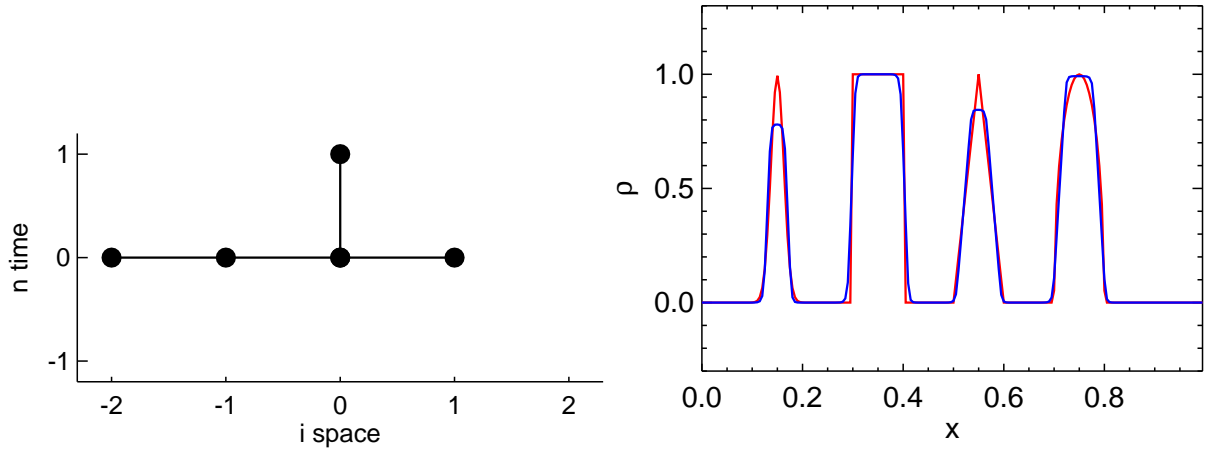


Figure 21: Stencil and example for PLM scheme with Superbee slope-limiter.

Figure 21: **PLM scheme** with **Superbee slope** (maximum allowed 2nd order slope).

$$\delta\rho_i = \left[\text{sign}(\rho_i - \rho_{i-1}) + \text{sign}(\rho_{i+1} - \rho_i) \right] \min \left(\text{abs}(\rho_i - \rho_{i-1}), \text{abs}(\rho_{i+1} - \rho_i), \frac{1}{2} \max(\text{abs}(\rho_i - \rho_{i-1}), \text{abs}(\rho_{i+1} - \rho_i)) \right). \quad (157)$$

2.6.9 PPM scheme

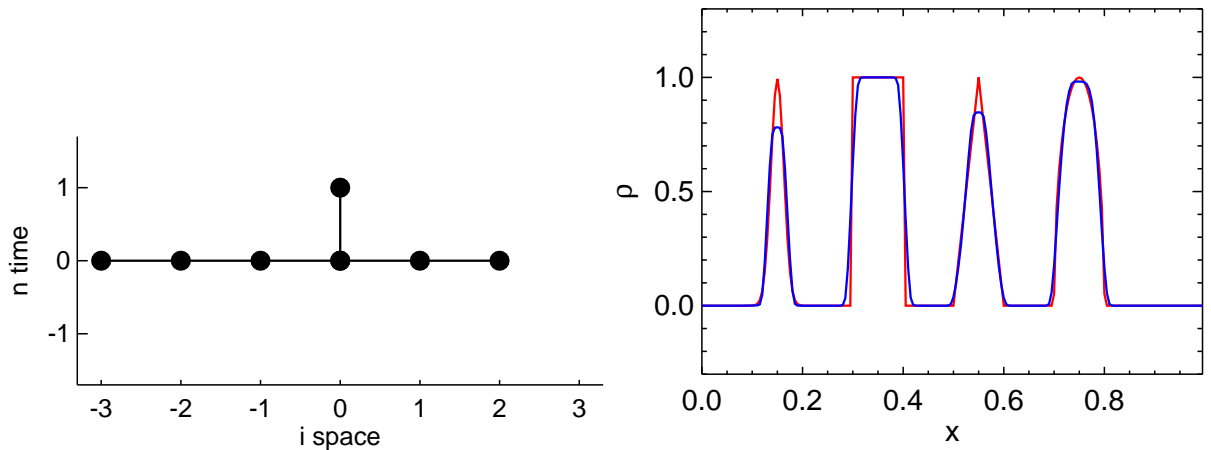


Figure 22: Stencil and example for PPM scheme.

Figure 22: **PPM scheme** with **piecewise parabolic reconstruction**. See Colella & Woodward (1984).

2.6.10 WENO scheme

Figure 23: **WENO scheme** with weighted essentially non-oscillatory reconstruction (with 6th order polynomials, without any Runge-Kutta sub-steps). See e.g. Jiang & Shu (1996).

2.6.11 Scheme with Superbee slope, only boundary value used

Figure 24: **Scheme** with **Superbee slope** where Eq. (148) was used for the flux instead of Eq. (147).

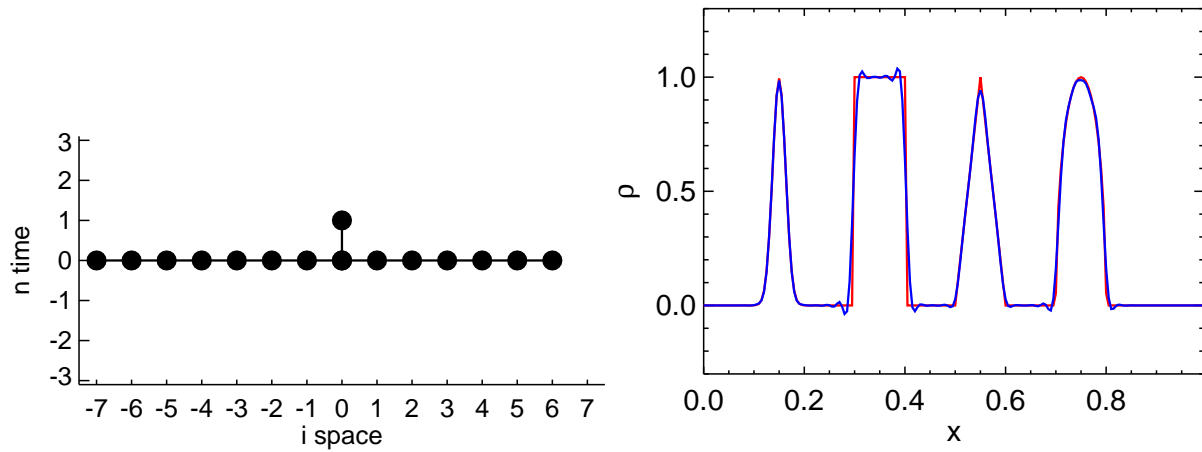


Figure 23: Stencil and example for WENO scheme.

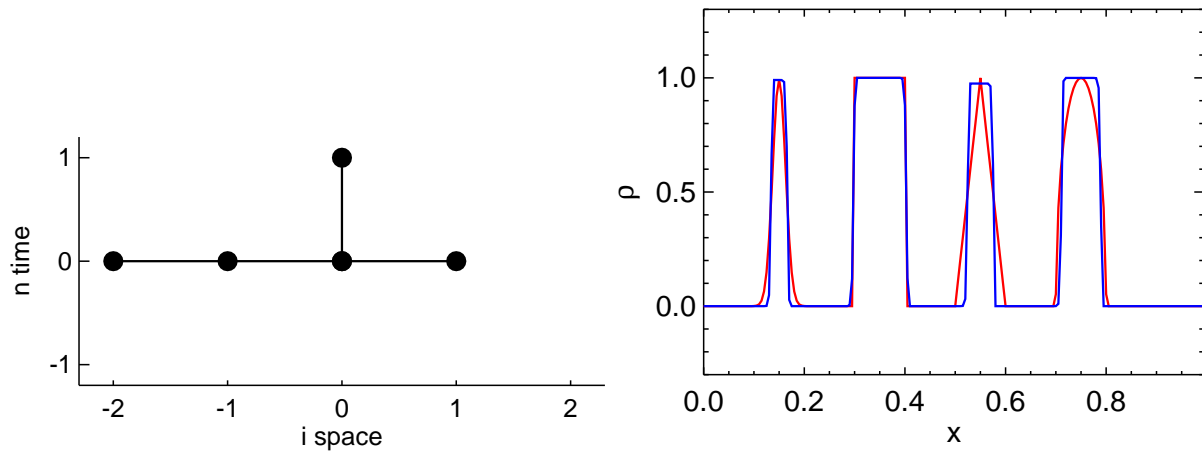


Figure 24: Stencil and example for modified scheme with Superbee slope.

2.6.12 Further improvements

- (W)ENO schemes can have very high order.
- (W)ENO schemes can be complemented by high-order Runge-Kutta steps.
- PPM: non-linear criteria can help to decide if e.g. shocks should be sharpened further.
- Subcell resolution can resolve the position of discontinuities within cells.

At some point only a finer grid helps:

- More grid points
- Non-equidistant grid
- Adaptively refined grid

3 Non-linear advection: Burgers' equation

3.1 Introduction of Burgers' equation

3.1.1 Viscous and inviscid Burgers' equation

Viscous Burgers' equation:

$$\frac{\partial v}{\partial t} + \frac{\partial \frac{1}{2}v^2}{\partial x} = \epsilon \frac{\partial^2 v}{\partial x^2} \quad (158)$$

inviscid **Burgers' equation** in conservation form (with flux $\frac{1}{2}v^2$)

$$\frac{\partial v}{\partial t} + \frac{\partial \frac{1}{2}v^2}{\partial x} = 0 \quad , \quad (159)$$

quasi-linear form

$$\frac{\partial v}{\partial t} + v \frac{\partial v}{\partial x} = 0 \quad , \quad (160)$$

and integral form

$$\int_{x_0}^{x_1} [v(x, t_1) - v(x, t_0)] dx + \int_{t_0}^{t_1} \left[\frac{1}{2}v^2(x_1, t) - \frac{1}{2}v^2(x_0, t) \right] dt = 0 \quad (161)$$

- It resembles the linear advection equation (63).
- However, it is **non-linear** with $v(x, t)$ instead of $v = \text{const.}$
- It describes the transport of v with velocity v .

3.1.2 Solution along characteristic curves

Characteristics already discussed for a quasi-linear PDE (Sect. 2.1.5).

Velocity v is not globally constant anymore.

However, it is constant along characteristic

$$c(t) = v(x_0) t + x_0 \quad . \quad (162)$$

That allows a graphical “solution” by using characteristics.

3.1.3 Compression waves and shocks

A **compression wave** with

$$\frac{\partial v}{\partial x} < 0 \quad (163)$$

steepens with time and characteristic curves can cross: multiple-valued solution?

- The viscous Burgers' equation (158) is a parabolic PDE and has a unique solution for all times $t > 0$.
- **Vanishing viscosity:** We look for a solution of the inviscid Burgers' equation that is a solution of the viscous Burgers' equation in the limit $\epsilon \rightarrow 0$.
- Instead of a multiple-valued solution we get a discontinuity where the characteristics end.
- **Discontinuities (shocks) are unavoidable** for $\frac{\partial v}{\partial x} < 0$.
- Characteristics run into a shock from both sides.
- Discontinuities should be allowed in the initial conditions.
- We need to find weak solutions.

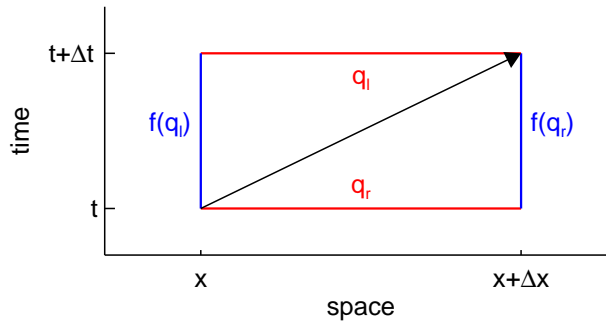


Figure 25: Jump across shock.

3.1.4 Shock speed I

A shock with speed s travels over an infinitesimal time Δt an infinitesimal distance

$$\Delta x = s \Delta t \quad (164)$$

(see Fig. 25). Integration of the PDE

$$\frac{\partial q}{\partial t} + \frac{\partial f(q)}{\partial x} = 0, \quad (165)$$

over Δt and Δx results in

$$\int_x^{x+\Delta x} [q(x, t + \Delta t) - q(x, t)] dx + \int_t^{t+\Delta t} [f(q(x + \Delta x, t)) - f(q(x, t))] dt = 0 \quad (166)$$

3.1.5 Shock speed II

During this time Δt the states q_l , q_r and fluxes $f(q_l)$, $f(q_r)$ on the left and right do not change (much) and we get

$$\Delta x q_l - \Delta x q_r + \Delta t f(q_r) - \Delta t f(q_l) = O(\Delta t^2) . \quad (167)$$

For $\Delta x = s \Delta t$ and $\Delta t \rightarrow 0$ we get the **Rankine-Hugoniot jump condition**

$$s (q_r - q_l) = f(q_r) - f(q_l) \quad (168)$$

which gives for the **shock speed** in general

$$s = \frac{f(q_r) - f(q_l)}{q_r - q_l} \quad (169)$$

and for Burgers' equation

$$s = \frac{\frac{1}{2}v_r^2 - \frac{1}{2}v_l^2}{v_r - v_l} = \frac{1}{2}(v_r + v_l) . \quad (170)$$

3.1.6 Expansion waves

Smooth regions with

$$\frac{\partial v}{\partial x} > 0 \quad (171)$$

produce a **rarefaction wave** or **expansion wave**.

- What about steps with $v_{\text{left}} < v_{\text{right}}$?
- Expansion shock with characteristics running out of it is weak solution.
- But: any small but non-zero viscosity would smooth the step and cause a rarefaction wave (or rarefaction fan).

- Only solutions that fulfil an **entropy condition** are allowed.

Lax entropy condition: For a convex scalar conservation law, a discontinuity propagating with speed s satisfies the Lax entropy condition if

$$v_{\text{left}} > s > v_{\text{right}} . \quad (172)$$

- Therefore: expansion shocks are not allowed.
- An entropy condition destroys time-reversibility.

3.1.7 Similarity solutions I

The quasi-linear PDE

$$\frac{\partial q}{\partial t} + \frac{df}{dq} \frac{\partial q}{\partial x} = 0 \quad (173)$$

for the **Riemann problem**

$$q(x, 0) = \begin{cases} q_l & \text{if } x < 0 \\ q_r & \text{if } x > 0 \end{cases} \quad (174)$$

has **similarity solutions** of the form

$$q(x, t) = \tilde{q}\left(\frac{x}{t}\right) . \quad (175)$$

3.1.8 Similarity solutions II

Inserting this ansatz (175) into Eq. (173) gives for $t > 0$

$$-\frac{x}{t^2} \tilde{q}' + \frac{df}{dq} \frac{1}{t} \tilde{q}' = 0 \quad (176)$$

with the solutions

$$\tilde{q}'\left(\frac{x}{t}\right) = 0 \Rightarrow \tilde{q}\left(\frac{x}{t}\right) = \text{const} \quad (177)$$

or

$$\tilde{q}'\left(\frac{x}{t}\right) \neq 0 \Rightarrow \frac{df}{dq}\left(\tilde{q}\left(\frac{x}{t}\right)\right) = \frac{x}{t} \quad (178)$$

which for Burgers' equation gives

$$v = \frac{x}{t} . \quad (179)$$

This solution (179) describes the state within a rarefaction fan whereas Eq. (177) applies everywhere else (outside of rarefaction waves and shocks).

3.1.9 Classification of Riemann problems

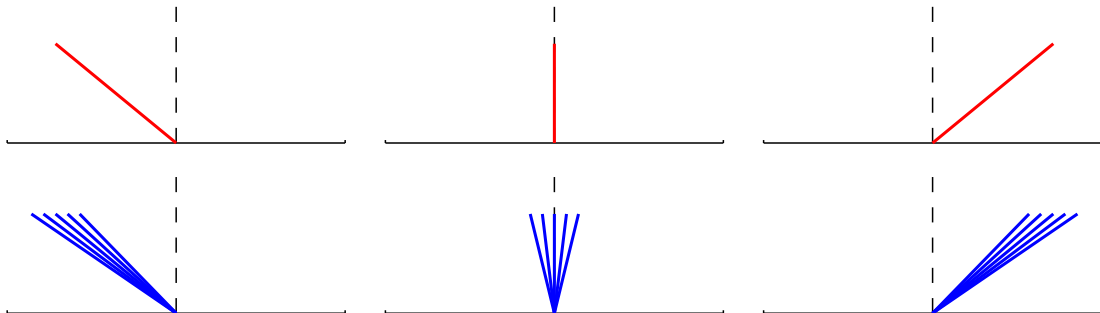


Figure 26: Different Riemann problems for Burgers' equation.

- A **Riemann problem** consists of a step at $x = 0$ in q with constant states q_l and q_r on the left and right side, see Eq. (174).
- Figure 26 shows different types of solutions with a **shock** (top) and a **rarefaction wave** (bottom).
- Except for the **transonic rarefaction wave** the flux across the boundary (dashed line) is either $f(q_l)$ or $f(q_r)$.

3.2 Numerical examples

3.2.1 Velocity at cell boundary

- With velocity possibly varying from cell to cell one needs to define an appropriate value at the cell boundary.

A logical choice is the shock speed from Eq. (169) which results in

$$v_{i+\frac{1}{2}} = \begin{cases} \frac{f(q_{i+1}^n) - f(q_i^n)}{q_{i+1}^n - q_i^n} & \text{if } q_{i+1}^n \neq q_i^n \\ \frac{df}{dq}(q_i^n) & \text{if } q_{i+1}^n = q_i^n \end{cases} \quad (180)$$

or for Burgers' equation from Eq. (170) simply

$$v_{i+\frac{1}{2}} = \frac{1}{2} (v_i^n + v_{i+1}^n) . \quad (181)$$

3.2.2 Flux-splitting

Both signs of the velocity are now possible.

Flux-splitting allows the use of schemes written for one sign of the velocity, still guaranteeing proper upwinding,

$$f(q) = f^+(q) + f^-(q) \quad (182)$$

with

$$\frac{df^+}{dq} \geq 0 , \quad \frac{df^-}{dq} \leq 0 . \quad (183)$$

E.g.: extension of FTBS scheme to **Courant-Isaacson-Rees scheme** (CIR, now stable for both signs of v):

$$f_{i+\frac{1}{2}}^n = \begin{cases} f(\rho_i^n) & \text{if } v_{i+\frac{1}{2}} > 0 \\ f(\rho_{i+1}^n) & \text{if } v_{i+\frac{1}{2}} \leq 0 \end{cases} \quad (184)$$

CIR for Burgers' equation:

$$f_{i+\frac{1}{2}}^n = \begin{cases} \frac{1}{2} (v_i^n)^2 & \text{if } v_{i+\frac{1}{2}} > 0 \\ \frac{1}{2} (v_{i+1}^n)^2 & \text{if } v_{i+\frac{1}{2}} \leq 0 \end{cases} \quad (185)$$

3.2.3 Example: small-amplitude wave

Even a small-amplitude wave that initially behaves like a linear wave (left panel in Fig. 27) turns later into a **shock wave** (right panel in Fig. 27).

3.2.4 Example: Gaussian and conservativity

Burgers' equation allows also the **non-conservative discretization** using upwind values

$$v_i^{n+1} = v_i^n - \frac{\Delta t}{\Delta x} v_i^n (v_i^n - v_{i-1}^n) \quad (186)$$

which results in the time-evolution in the left panel in Fig. 28.

The right panel shows the result with the conservative scheme (185).

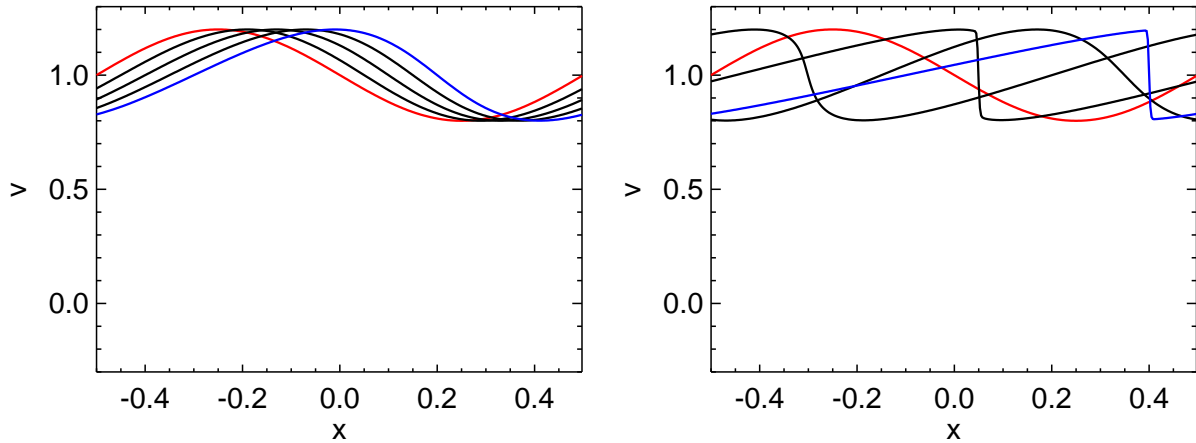


Figure 27: Small-amplitude wave: linear behaviour (left), shock wave (right).

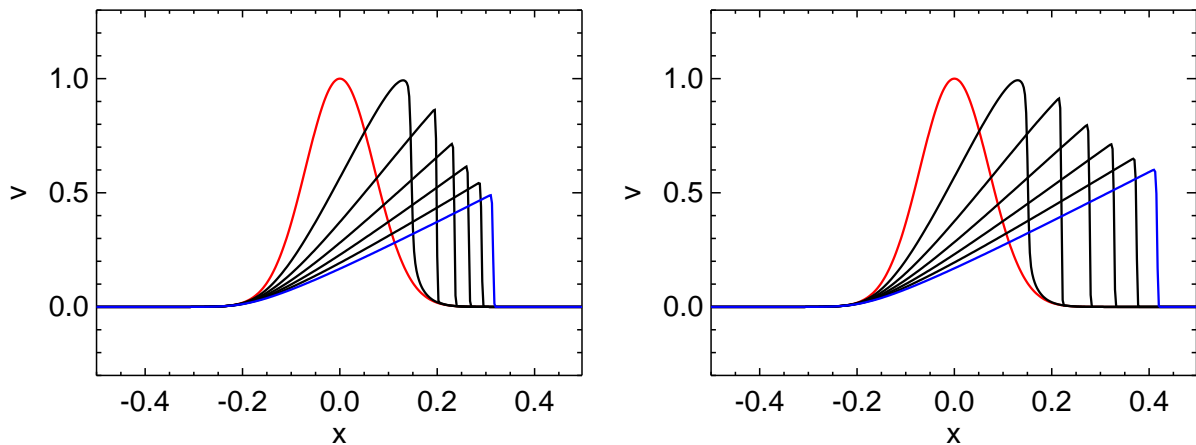


Figure 28: Non-conservative scheme (left), conservative scheme (right).

3.2.5 Lax-Wendroff theorem

- The initial evolution of the schemes (Fig. 28) is rather similar.
- However, with the non-conservative scheme, the shock moves with the wrong speed and the non-conservation of the area under v is obvious.
- Remember: the derivation of the Rankine-Hugoniot jump condition in Sect. 3.1.5 used the conservation of q across the shock to derive the shock speed.

Lax-Wendroff theorem: If the numerical solution of a conservative scheme converges, it converges towards a weak solution.

- Note: an alternative to [shock capturing](#) where the scheme itself is able to handle discontinuities is [shock tracking](#) where the positions of shocks are explicitly followed to allow a different numerical treatment in smooth regions and near discontinuities.

3.2.6 Example: step-function and conservativity

Figure 29 displays the outcome for a test with an initial step-function (a Riemann problem) for the non-conservative scheme (186) and the conservative scheme (185).

- Clearly, the non-conservative scheme **fails again to get the shock speed right**.
- The wrong solution is not indicated by any helpful wiggles or numerical artifacts.

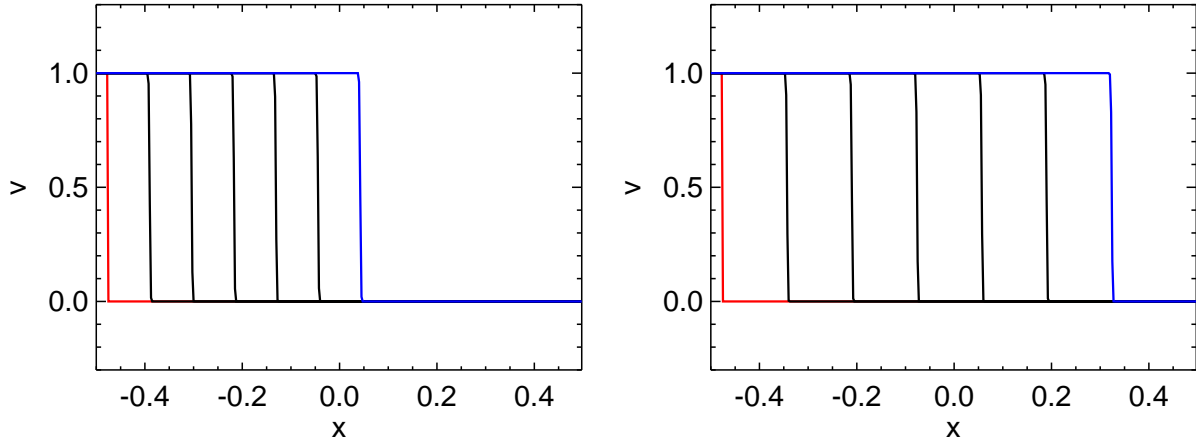


Figure 29: Non-conservative scheme (left), conservative scheme (right).

3.2.7 Example: expansion shock and rarefaction fan

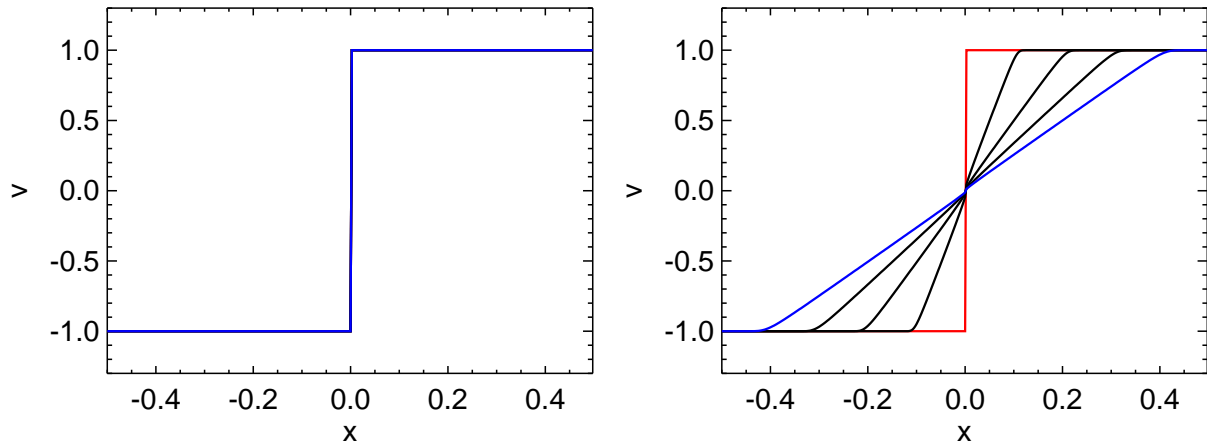


Figure 30: Expansion shock (left) and – correct – rarefaction fan (right).

The Riemann problem in Fig. 30 should result in a **rarefaction fan** (right panel).

- Instead, the CIR scheme from Eq. (185) produces a stationary **expansion shock** that violates the entropy condition (172).
- The solution by the CIR scheme is stationary because its flux ($f = \frac{1}{2}$) is the same everywhere, even if the velocity ($v = \pm 1$) changes sign.

3.2.8 Entropy production by artificial viscosity

A possibly way to prevent the violation of the entropy condition (172) is to produce entropy with an extra **(artificial) diffusion term** added to the CIR flux (185) according to

$$f_{i+\frac{1}{2}}^n = f_{i+\frac{1}{2}}^n(\text{CIR}) - \epsilon (v_{i+1}^n - v_i^n) . \quad (187)$$

However, now the parameter ϵ has to be tuned to be large enough to give the correct weak solution while not smearing it more than necessary.

The viscosity parameter ϵ could be replaced e.g. by the function

$$\epsilon = \epsilon' (v_{i+1}^n - v_i^n)^2 \quad (188)$$

to confine the extra viscosity to regions where the gradient is really large.

3.2.9 Entropy fix

- For most Riemann problems (Fig. 26) the CIR scheme (185) actually produces initially the exact result.
- Only for a transonic rarefaction wave (as in the last example in Fig. 30) it differs.
- **Godunov's idea:** Solve a Riemann problem (\Rightarrow [Riemann solver](#)) at every cell boundary and derive the corresponding flux over the boundary.
- For Burgers' equation the flux through the stagnation point ($v = 0$) in a transonic rarefaction wave is $f = \frac{1}{2}v^2 = 0$.

\Rightarrow Extend the CIR scheme to get a **Godunov-type scheme** by defining

$$f_{i+\frac{1}{2}}^n = \begin{cases} \frac{1}{2} (v_i^n)^2 & \text{if } v_{i+\frac{1}{2}} > 0 \text{ and } v_i \geq 0 \\ \frac{1}{2} (v_{i+1}^n)^2 & \text{if } v_{i+\frac{1}{2}} \leq 0 \text{ and } v_{i+1} \leq 0 \\ 0 & \text{if } v_i < 0 < v_{i+1} \end{cases} \quad (189)$$

The additional branch is an **entropy fix** to the CIR scheme.

3.2.10 Concepts from the linear world

- Consistency: the same
- Conservativity: the same (now even more important)
- Stability
 - Linear stability: not directly applicable (linearization possible?)
 - Total variation diminishing (TVD): applicable
 - Alternative: base scheme on concepts that work in the linear case and perform lots of tests for the non-linear PDE
- Accuracy: slope-limiter schemes need adaption

3.2.11 Transformation of shock speed formula

Velocity at cell boundary from shock speed (Eq. (169) and Eq. (180), entropy fix ignored),

$$v_{i+\frac{1}{2}} = \frac{f(q_{i+1}^n) - f(q_i^n)}{q_{i+1}^n - q_i^n} \quad (190)$$

$$= \frac{f(q_{i+1}^n) - \frac{f(q_i^n) + f(q_{i+1}^n)}{2}}{q_{i+1}^n - \frac{q_i^n + q_{i+1}^n}{2}} = \frac{f(q_i^n) - \frac{f(q_i^n) + f(q_{i+1}^n)}{2}}{q_i^n - \frac{q_i^n + q_{i+1}^n}{2}} \quad (191)$$

$$= \frac{f\left(q_{i_{\text{up}} i+\frac{1}{2}}^n\right) - \frac{f(q_i^n) + f(q_{i+1}^n)}{2}}{q_{i_{\text{up}} i+\frac{1}{2}}^n - \frac{q_i^n + q_{i+1}^n}{2}} \quad (192)$$

with the upwind index

$$i_{\text{up} i+\frac{1}{2}} := \begin{cases} i & \text{if } v_{i+\frac{1}{2}} > 0 \\ i + 1 & \text{if } v_{i+\frac{1}{2}} \leq 0 \end{cases} \quad (193)$$

3.2.12 Second-order extension of flux formula

Resolving Eq. (192) for the upwind flux that we need as flux (184) for the CIR scheme gives

$$f_{i+\frac{1}{2}}^n = f\left(q_{i_{\text{up}}i+\frac{1}{2}}^n\right) = \underbrace{\frac{f(q_i^n) + f(q_{i+1}^n)}{2}}_{\text{flux average}} + v_{i+\frac{1}{2}} \underbrace{\left(q_{i_{\text{up}}i+\frac{1}{2}}^n - \frac{q_i^n + q_{i+1}^n}{2}\right)}_{\text{linear(ized) advection}}. \quad (194)$$

Remember: This is exactly the simple upwind (CIR) flux.

However, the second term looks like linear advection and suggests to apply a **higher-order (eg. slope-limiter) scheme** to the **localized advection problem** for

$$q'_j = q_j - \frac{q_i + q_{i+1}}{2} \quad \text{for } j = i-1, i, i+1, i+2. \quad (195)$$

4 One-dimensional non-linear hydrodynamics

4.1 New Difficulties

4.1.1 A coupled non-linear system

- The 1D hydrodynamics equations (40) are a non-linear system of 3 **coupled equations**.
- There is a little bit from the linear advection equation:
 - Derivation of the characteristic form (48).
 - Linear advection as special case (see Sect. 2.1.3).
- There is a little bit from Burgers' equation:
 - Shocks can arise from smooth initial conditions.
 - Discontinuities in the initial conditions can produce rarefaction waves.
 - We need to look for weak solutions (that satisfy an entropy condition).
- Characteristics are not necessarily straight lines.
- The domain of dependence is not only a single point but an interval. However, it is bounded. Therefore explicit methods (with limited full numerical domain of dependence) are often adequate.

4.1.2 Positivity of density

To compute the velocity from momentum and density via

$$v = \frac{\rho v}{\rho} \quad (196)$$

requires

$$\rho > 0 . \quad (197)$$

An **overshoot of the density to non-positive values** is now (usually) disastrous.

4.1.3 Positivity of pressure

The pressure $P(e_i, \rho)$ depends on the conserved quantities via

$$P(\rho, \rho v, \rho e_{ik}) = P\left(\frac{\rho e_{ik}}{\rho} - \frac{(\rho v)^2}{2\rho^2}, \rho\right) . \quad (198)$$

An overshoot in velocity may lead to **negative pressure** (or an attempt to access values beyond the limits of a tabulated equation of state).

- This restriction is so severe that in some cases the conservation of total energy might be given up in favor of a (non-conservative) formulation where the positivity of the internal energy is guaranteed.
- The total variation of e.g. density, pressure, ... of the true solution can increase $\rightarrow TV$ stability arguments no longer hold.

4.1.4 Where is upwind?

Bringing the Euler equations into characteristic form resulted in waves with different velocities (Sect. 1.5.4),

$$v - c, \quad v, \quad v + c . \quad (199)$$

Which one should be used to determine the **upwind direction**?

4.2 The Riemann problem for the 1D Euler equations

4.2.1 The Riemann problem

The state on each side described by 3 values.

Each wave family can cause a discontinuity:

- Sound waves can cause shocks or rarefaction waves.
- The material flow (entropy wave) can have a contact discontinuity.

The solution of Riemann problem (for convex – simple – EOS) can comprise:

- 0 or 1 contact discontinuity,
- 0, 1, or 2 shocks,
- 0, 1, or 2 rarefaction waves; not more than 2 (shocks + rarefaction waves).

4.2.2 Rankine-Hugoniot conditions

The **Rankine-Hugoniot jump conditions** (see Sect. 3.1.5) for the 1D Euler equations (40), describing a shock with speed s become

$$s (\rho_r - \rho_l) = \rho v_r - \rho v_l \quad (200)$$

$$s (\rho v_r - \rho v_l) = (\rho v v + P)_r - (\rho v v + P)_l \quad (201)$$

$$s (\rho e_{ikr} - \rho e_{ikl}) = ([\rho e_{ik} + P] v)_r - ([\rho e_{ik} + P] v)_l \quad (202)$$

They can only be fulfilled for certain combinations of q_l and q_r .

An arbitrary Riemann problem typically causes more than one jump.

4.2.3 Example: Sod shock tube

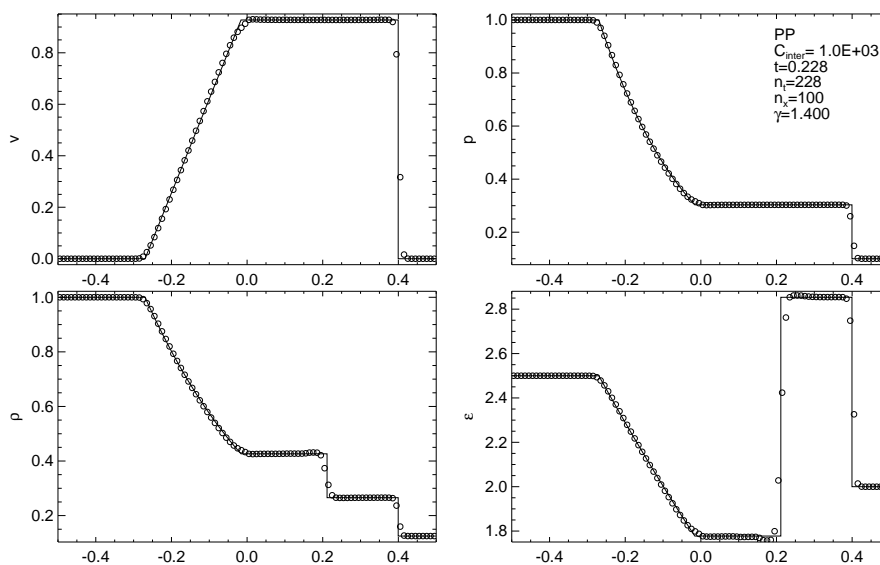


Figure 31: Sod shock tube: analytical (lines) and numerical (circles) solution. Velocity, pressure, density, internal energy.

The **Sod shock tube** (Fig. 31) is a Riemann problem with:
 $(\rho, P, v)_l = (1, 1, 0)$, $(\rho, P, v)_r = (1/8, 1/10, 0)$.

4.2.4 Jumps in the solution of the Sod shock tube problem

The similarity solution of the Sod shock tube problem contains

- a **rarefaction wave** going to the left,
- a **contact discontinuity** travelling slowly to the right,
- a **shock wave** moving fast to the right.

For the all individual waves the upwind direction is clear.

Only in the (possible) case of a transonic rarefaction wave “upwind” is not obvious. However, here an entropy fix has to be applied, anyway.

4.3 Riemann solvers

4.3.1 Godunov-type schemes

Godunov’s idea: solve a separate Riemann problem at each cell boundary (Fig. 32). **RSA**: three

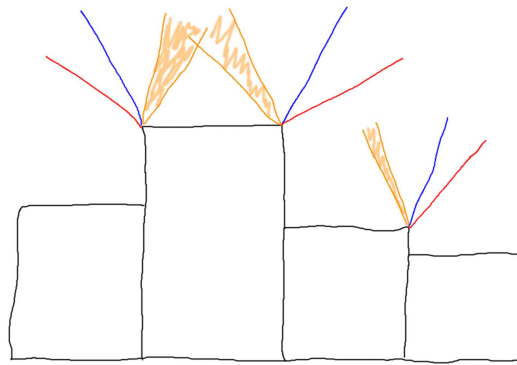


Figure 32: Many Riemann problems.

steps:

- **Reconstruct** $\rho(x)$, $\rho\mathbf{v}(x)$, $\rho e_{ik}(x)$ from ρ_i , $\rho\mathbf{v}_i$, ρe_{ik_i} (constant values within cell).
- **Solve** the Riemann problems for Δt (and compute fluxes across cell boundaries).
- **Average** $\rho(x)$, $\rho\mathbf{v}(x)$, $\rho e_{ik}(x)$ to get ρ_i , $\rho\mathbf{v}_i$, ρe_{ik_i} (apply the conservative update formula).

The concept is very useful, but the scheme is too diffusive in its original form.

4.3.2 Riemann solvers and higher-order schemes

Combination of Godunov’s concept (local solution of **fully non-linear Riemann solvers**) with **high-order reconstruction** (solution averaging):

- Godunov (1959): Exact Riemann solver (with **constant** reconstruction)
- Van Leer (1979): **MUSCL** (Monotone Upwind Schemes for Scalar Conservation Laws): **linear** reconstruction: approximation of piecewise-linear Riemann problems by piecewise-constant Riemann problems including slope-limiter, solution of the Lagrange equations, Eulerian remapping.
- Colella & Woodward (1984): **PPM** (Piecewise Parabolic Method): **piecewise parabolic** reconstruction via primitive functions, contact steepening.

Godunov-type schemes are conceptionally appealing.

The improved high-resolution methods give excellent results.

- However, they are relatively complex and require a lot of operations per grid cell.
- Approximate (linearized) Riemann solvers may serve as well in splitting the flow into waves with different characteristic velocities and upwind directions.

4.4 Approximate (linear) Riemann solvers

4.4.1 Linearized flux

A linearized Riemann solver uses a linearization of the vector flux \mathbf{F} in Eq. (41) around reference value \mathbf{q}_{ref} to bring it into a form similar to the scalar Eq. (194),

$$\mathbf{F} = \mathbf{F}(\mathbf{q}_{\text{ref}}) + \frac{\partial \mathbf{F}}{\partial \mathbf{q}}(\mathbf{q}_{\text{ref}}) (\mathbf{q} - \mathbf{q}_{\text{ref}}) + O\left((\mathbf{q} - \mathbf{q}_{\text{ref}})^2\right) . \quad (203)$$

Dropping the 2nd order term and choosing $x_{\text{ref}} = x_{i+\frac{1}{2}}$ we get

$$\mathbf{q}_{\text{ref}} = \mathbf{q}_{i+\frac{1}{2}} \sim \frac{1}{2} (\mathbf{q}_i + \mathbf{q}_{i+1}) , \quad (204)$$

$$\mathbf{F}(\mathbf{q}_{\text{ref}}) \sim \frac{1}{2} (\mathbf{F}(\mathbf{q}_i) + \mathbf{F}(\mathbf{q}_{i+1})) . \quad (205)$$

We remember from Sect. 1.5.3 that for the Jacobian

$$\bar{\bar{A}}_{i+\frac{1}{2}} := \frac{\partial \mathbf{F}}{\partial \mathbf{q}}(\mathbf{q}_{\text{ref}}) \quad (206)$$

there is a matrix $\bar{\bar{Q}}_{i+\frac{1}{2}}$ that brings it into diagonal form

$$\bar{\bar{A}}_{i+\frac{1}{2}} = \bar{\bar{Q}}_{i+\frac{1}{2}}^{-1} \bar{\bar{A}}_{i+\frac{1}{2}} \bar{\bar{Q}}_{i+\frac{1}{2}} , \quad \bar{\bar{A}}_{i+\frac{1}{2}} = \bar{\bar{Q}}_{i+\frac{1}{2}} \bar{\bar{\Lambda}}_{i+\frac{1}{2}} \bar{\bar{Q}}_{i+\frac{1}{2}}^{-1} . \quad (207)$$

4.4.2 Linearized Riemann solver

The linearized flux vector becomes

$$\mathbf{F}_{i+\frac{1}{2}} = \underbrace{\frac{\mathbf{F}(\mathbf{q}_i) + \mathbf{F}(\mathbf{q}_{i+1})}{2}}_{\text{centered (naive) fluxes}} + \bar{\bar{Q}}_{i+\frac{1}{2}} \bar{\bar{\Lambda}}_{i+\frac{1}{2}} \underbrace{\left[\bar{\bar{Q}}_{i+\frac{1}{2}}^{-1} \left(\mathbf{q} - \frac{\mathbf{q}_i + \mathbf{q}_{i+1}}{2} \right) \right]}_{\substack{\text{original fluctuations} \\ \text{fluctuations of characteristic waves} \\ \text{fluxes of characteristic waves} \\ \text{flux corrections}}} \quad (208)$$

Note: $\bar{\bar{\Lambda}}_{i+\frac{1}{2}}$ is a diagonal matrix with the characteristic velocities on the diagonal.

Note: The fluxes of the characteristic waves are the result of a localized linear advection problem. A higher-order correction term (with slope-limiter) could be applied.

4.4.3 Examples of schemes

Roe (1981):

- Scheme (essentially) as above.
- With clever choice of matrix A , so that the approximate Riemann solver becomes exact for simple waves (only one shock or only one contact discontinuity).
- Needs entropy fix.
- The fluctuations are taken from the primitive rather than the conservative variables.

HLLE (1983, 1988):

- Uses only the two waves with largest and smallest characteristic velocity.
- The region in between is approximated by a single state.
- The scheme is simple, more robust but also more dissipative than Roe's scheme.

4.4.4 Example: Sod shock tube with Roe solver, constant

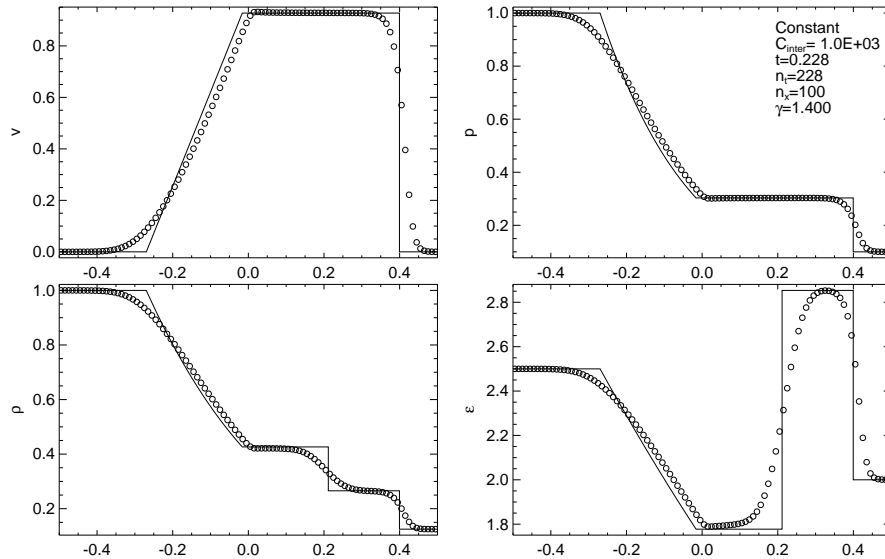


Figure 33: Sod shock tube: constant reconstruction.

Figure 33: numerical solution of the **Sod shock tube** problem with **constant reconstruction**.

4.4.5 Example: Sod shock tube with Roe solver, Minmod slope

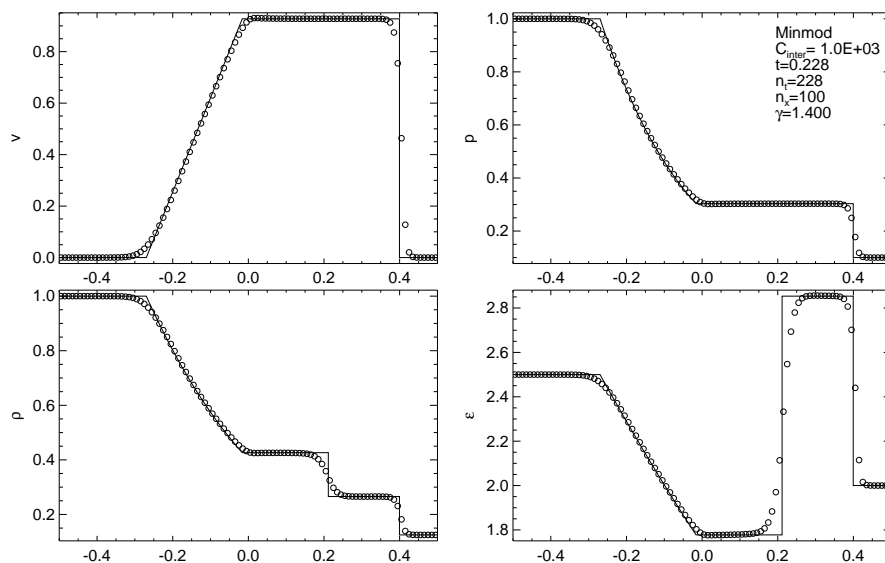


Figure 34: Sod shock tube: Minmod slope-limiter.

Figure 34: numerical solution of the **Sod shock tube** problem with **PL reconstruction** and **Minmod slope-limiter**.

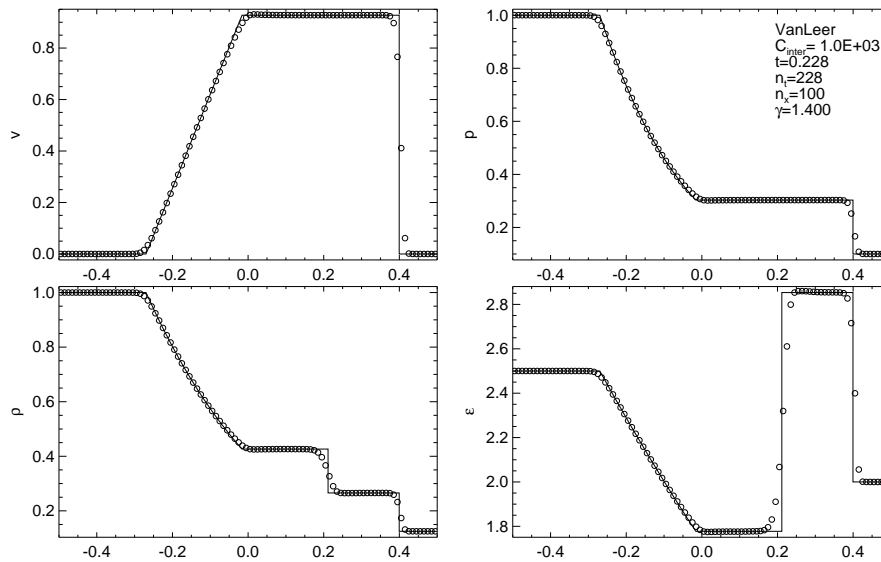


Figure 35: Sod shock tube: vanLeer slope-limiter.

4.4.6 Example: Sod shock tube with Roe solver, vanLeer slope

Figure 35: numerical solution of the **Sod shock tube** problem with **PL reconstruction** and **vanLeer slope-limiter**.

4.4.7 Example: Sod shock tube with Roe solver, Superbee slope

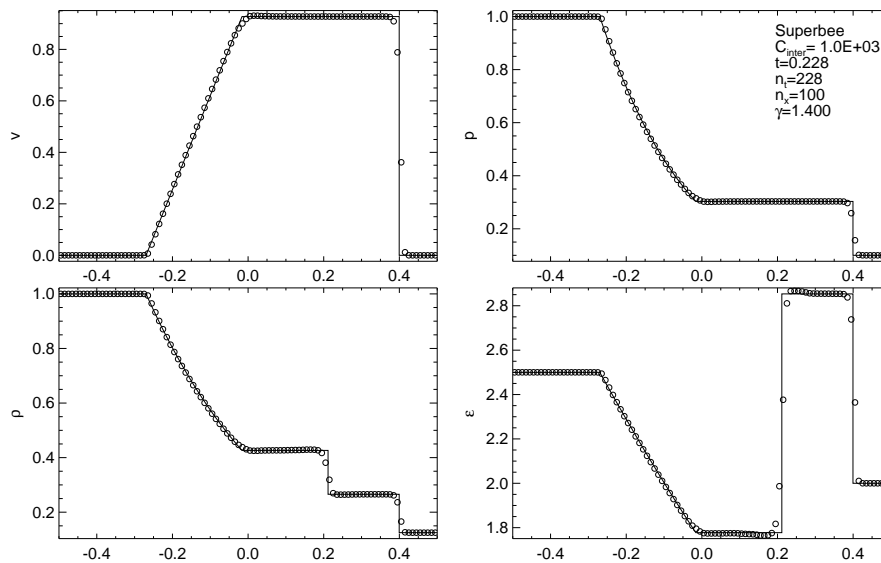


Figure 36: Sod shock tube: Superbee slope-limiter.

Figure 36: numerical solution of the **Sod shock tube** problem with **PL reconstruction** and **Superbee slope-limiter**.

4.4.8 Example: Sod shock tube with Roe solver, PP reconstruction

Figure 37: numerical solution of the **Sod shock tube** problem with **PP reconstruction**.

4.5 Alternative concepts

(Approximate) Riemann solvers are a way to account for upwinding and shock capturing in a conceptually elegant manner.

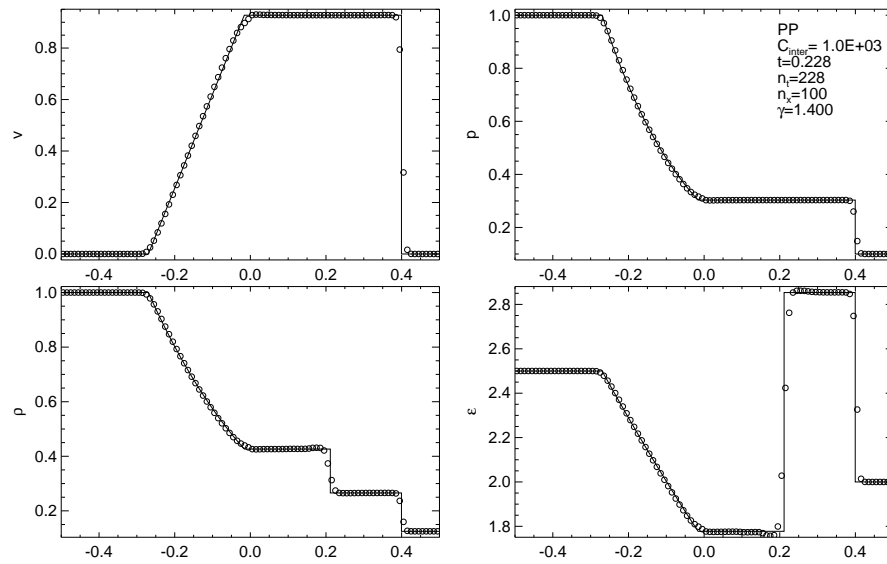


Figure 37: Sod shock tube: PP reconstruction.

However, they are somewhat involved and there other (simpler? older?) concepts around, which make use of

- von Neumann-Richtmyer viscosity
- Runge-Kutta steps
- operator-splitting of advection and pressure terms

5 Applications

5.1 Composing operators

5.1.1 Operator adding versus splitting

Let the time evolution of q be determined by two operators A and B according to

$$\frac{dq}{dt} = A(q) + B(q) . \quad (209)$$

Suppose there are separate numerical schemes available that allow to compute the individual updates

$$q_A^{n+1} = q^n + \Delta t A(q^n) , \quad q_B^{n+1} = q^n + \Delta t B(q^n) . \quad (210)$$

Now, the two schemes could be combined in two ways, e.g. by **operator adding**

$$q_{A+B}^{n+1} = q^n + \Delta t A(q^n) + \Delta t B(q^n) \quad (211)$$

or **Godunov operator splitting**

$$\begin{aligned} q_A^{n,*} &= q^n + \Delta t A(q^n) \\ q_{A+B}^{n+1} &= q_A^{n,*} + \Delta t B(q_A^{n,*}) . \end{aligned} \quad (212)$$

The results are generally not the same. Both methods have advantages/drawbacks.

5.1.2 Godunov versus Strang operator splitting

The Godunov operator splitting from Eq. (212) where all operators are applied cyclically and with the same time-step might be improved in some cases by **Strang operator splitting**

$$\begin{aligned} q_{A/2}^{n,*} &= q^n + \frac{\Delta t}{2} A(q^n) \\ q_{A/2+B}^{n,**} &= q_{A/2}^{n,*} + \Delta t B(q_{A/2}^{n,*}) \\ q_{A+B}^{n+1} &= q_{A/2+B}^{n,**} + \frac{\Delta t}{2} A(q_{A/2+B}^{n,**}) . \end{aligned} \quad (213)$$

5.1.3 Steady-state solutions with operator adding or splitting

Suppose both operators A and B are zero,

$$A = B = 0 \quad (214)$$

resulting in individually **stationary solutions** (eg. hydrostatic and radiative equilibrium),

$$q_A^{n+1} = q^n , \quad q_B^{n+1} = q^n , \quad (215)$$

which gives for both operator combination methods

$$q_{A+B}^{n+1} = q^n . \quad (216)$$

However, if the individual operators are non-zero but cancel each other,

$$B = -A \neq 0 \quad (217)$$

the adding of the operator gives equilibrium Eq. (216), while operator splitting

$$\begin{aligned} q_A^{n,*} &= q^n + \Delta t A(q^n) \\ q_{A+-A}^{n+1} &= q_A^{n,*} - \Delta t A(q_A^{n,*}) . \end{aligned} \quad (218)$$

This is not necessarily a stationary solution. Here, operator adding is superior.

5.1.4 Linear stability of operator adding or splitting

If both operators A and B are linear with amplification factors indicating stability

$$V_A \leq 1, \quad V_B \leq 1 \quad (219)$$

then the amplification factor of the scheme combined by operator splitting is

$$V_{A+B} = V_A V_B \leq 1 \quad (220)$$

implying **stability of the combined scheme**.

The adding of the operators requires a re-analysis of the combined scheme. It might be stable or not, even if Eq. (219) applies.

The individual analysis of a non-linear hydrodynamics and a complex non-local radiation transport scheme is difficult enough. It is convenient to have a combination method, that – at least in some simple cases – guarantees the stability of the combination

Here, operator splitting is superior.

5.1.5 Going multi-dimensional

Directional splitting or **dimensional splitting** is simply the technique to apply operator splitting to the spatial derivatives in the Euler equations:

$$\frac{\partial}{\partial t} \mathbf{q} + \frac{\partial}{\partial x} \mathbf{F}(\mathbf{q}) + \frac{\partial}{\partial y} \mathbf{F}(\mathbf{q}) = \mathbf{0} \quad (221)$$

becomes

$$\begin{aligned} q_{X,i}^{n,*} &= q_i^n - \frac{\Delta t}{\Delta x} \left(f\left(q_{i+\frac{1}{2}}^n\right) - f\left(q_{i-\frac{1}{2}}^n\right) \right) \\ q_{X+Y,i}^{n+1} &= q_{X,i}^{n,*} - \frac{\Delta t}{\Delta y} \left(f\left(q_{X,i+\frac{1}{2}}^{n,*}\right) - f\left(q_{X,i-\frac{1}{2}}^{n,*}\right) \right) . \end{aligned} \quad (222)$$

Directional splitting in general works very well and allows the application of powerful algorithms developed for 1D problems.

However, there are cases when a small amount of additional multi-dimensional tensor viscosity is necessary to damp spurious oscillations (even with PPM scheme).

5.2 Coupling of hydrodynamics and radiation transport

5.2.1 Coupling

If possible one would try to avoid constructing a merged hydrodynamics plus radiation transport scheme.

Instead one constructs and tests a hydrodynamics and a radiation transport scheme separately.

The **coupling can be done via operator splitting** or adding.

Often radiation transport requires small time-steps to achieve stability.

These can be handled by

- sub-steps for the radiation transport (many small radiation steps per large hydrodynamics step)
- or by an implicit treatment of the radiation transport (while the hydrodynamics operator is still explicit).

5.2.2 Stability requirements

Stability requirements on radiation transport operator:

1. Stability of integration along ray (to avoid problems like in Sect. 2.2.2)
2. Stability of (accelerated) Λ iteration
3. Stability of time-update

Note: Requirement 2 does not occur if the source function is independent of intensity (LTE).

Note: Requirement 1 does not occur if e.g. diffusion approximation is used.

Note: Requirement 3 is always there.

Sub-steps
time-step control

5.2.3 Approximations

Simplified treatment of radiative energy transfer during the simulation:

- Ignoring of radiation.
- Isothermal flow (no energy transport equation).
- Local cooling (in the optically thin).
- Diffusion approximation (in the optically thick).
- Non-local radiation transport along rays, but LTE and grey opacities.
- Non-local radiation transport along rays, but LTE and binned opacities (ODFs).

More sophisticated a posteriori radiation transport for spectrum synthesis.

5.3 Improvements

5.3.1 Non-Cartesian and/or refined grids

Possible numerical grid improvement techniques:

- Eulerian \rightarrow Lagrangian
- Equidistant \rightarrow non-equidistant
- Structured \rightarrow unstructured
- One \rightarrow many hierarchical
- Fixed in time \rightarrow adaptive
- Grid \rightarrow no grid: SPH

5.3.2 Optimization strategies

All modern computers can calculate (within the processor) much faster than they can access external memory.

Techniques to improve the performance of algorithms have to take this into account (simplified crash course):

- Efficient use of registers: Lots of operations with the same scalars are good.
- Cache optimization: Lots of operations with the same vectors are good.

- Vectorization (on dedicated vector machines or PCs): “Smooth” access to arrays and simple operations are good.
- Parallelization: Local access to array regions is good.

Hydrodynamics and parallelization:

- A bounded numerical domain of dependence allows straightforward domain decomposition and distribution over different machines.

Radiation transport and parallelization:

- Non-local radiation transport (integration along rays) requires more communication between processors and limits the performance on parallel computers.

A Nomenclature

A.1 Quantities

symbol	quantity
Δt	discrete time-step
Δx	grid size
e_i	internal energy density (per mass unit)
e_{ik}	total (internal + kinetic) energy
e_{ikg}	total (internal + kinetic + potential) energy
e_{ikb}	total (internal + kinetic + magnetic) energy
I_ν	frequency-dependent intensity
$\hat{\mathbf{n}}$	normal vector of length unity
ν	frequency
P	pressure
ρ	mass density
ρe_i	internal energy density (per volume)
$\bar{\mathbb{I}}$	unity tensor
\mathbf{v}	velocity vector

Table 1: Symbols and descriptions for quantities.

A.2 Vector notation

vector operation	description
$s s \rightarrow s$	product of scalars
$s \mathbf{v} \rightarrow \mathbf{v}$	scalar times vector gives vector
$\mathbf{v} s \rightarrow \mathbf{v}$	
$s \bar{\mathbb{T}} \rightarrow \bar{\mathbb{T}}$	scalar times tensor gives tensor
$\bar{\mathbb{T}} s \rightarrow \bar{\mathbb{T}}$	
$\mathbf{v} \cdot \mathbf{v} \rightarrow s$	scalar product of vectors gives scalar
$\mathbf{v} : \mathbf{v} \rightarrow \bar{\mathbb{T}}$	tensor product of vectors gives tensor
$\bar{\mathbb{T}} \mathbf{v} \rightarrow \mathbf{v}$	tensor times vector gives vector
$\mathbf{v} \cdot \bar{\mathbb{T}} \rightarrow \mathbf{v}^T$	“scalar product” of vector and tensor gives “transposed” vector
$\bar{\mathbb{T}} \bar{\mathbb{T}} \rightarrow \bar{\mathbb{T}}$	tensor product (“matrix multiplication”)
$\mathbf{v} \mathbf{v} \rightarrow ???$	

Table 2: Vector notation for scalar s , vector \mathbf{v} , and second-rank tensor $\bar{\mathbb{T}}$.

B Schedule

- Lecture 1: Monday, 2010-01-25, Sect. 1.1.1

C References

C.1 Lecture Notes

Lecture Notes closely related to the current one:

- Rony Keppens: “Introduction to computational magneto-fluid dynamics, with astrophysical applications”
- Anthony Mezzacappa: “Computational Fluid Dynamics for Astrophysics”
- Ewald Müller: “Les simulations numériques : une revue des différentes techniques et de leurs applications” (English)
- Claus-Dieter Munz: “Numerical Gasdynamic”
- Paul Ricker: “Computational Astrophysics and Cosmology”

Lecture Notes with additional topics:

- Ewald Müller, Friedrich Kupka: “Einführung in die theoretische Astrophysik” (German)
- Cole Miller: “Theoretical Astrophysics”
- M. Manzini: “Numerical methods for 1D compressible flows, an interactive book”
- James R. Graham: “Astrophysical Gas Dynamics”
- Wilhelm Kley, Jochen Peitz: “Theoretische Astrophysik” (German)
- Kip Thorne: “Applications of Classical Physics”
- Axel Brandenburg: “Computational aspects of astrophysical MHD and turbulence”, see here also
- Michel Rieutord: “Fondements de la dynamique des fluides et prolongements vers la convection thermique” (French)

C.2 Books

- Ferziger, J.H., Peric, M. 2001, “Computational Methods for Fluid Dynamics”, Springer-Verlag, ISBN: 3540420746
- Laney, C.B. 1998, “Computational Gasdynamics”, Cambridge University Press, ISBN: 0521625580
- LeVeque, R.J. 2002, “Finite Volume Methods for Hyperbolic Problems”, Cambridge University Press, ISBN: 0521009243
- LeVeque, R.J., Steiner, O., Gauthier, A. 1997, “Computational Methods for Astrophysical Fluid Flow (Saas-Fee Advanced Course...Lecture Notes)”, Springer-Verlag, ISBN: 3540644482
- Tannehill, J.C., Anderson, D.A., Pletcher, R.H. 1984/1997, “Computational Fluid Mechanics and Heat Transfer”, Taylor and Francis, ISBN: 1-56032-046-X

C.3 Articles

- Phillip Colella, Paul R. Woodward 1984, “The Piecewise Parabolic Method (PPM) for Gas-Dynamical-Simulations”, JCP 54, 174-201
- S.K. Godunov 1959, “A Difference Scheme for Numerical Computation of Discontinuous Solutions of Hydrodynamics Equations”, Math. Sbornik 47, 271-306
- Guang-Shan Jiang, Chi-Wang Shu 1996, “Efficient Implementation of Weighted ENO Schemes”, JCP 126, 202-228, see CiteSeer
- Bram van Leer 1979, “Towards the Ultimate Conservative Difference Scheme. V. A Second-Order Sequel to Godunov’s Method”, JCP 32, 101-136
- P.L. Roe 1981, “Approximate Riemann Solvers, Parameter Vectors, and Difference Schemes”, JCP 43, 357-372

C.4 Hydrodynamic codes

- List of “Free and Low-Cost CFD Software”
- List of existing Astrophysical Hydrodynamics Code Packages
- CFD codes list - free software
- CLAWPACK
- CLAWPACK
- CO5BOLD (non-public)
- COSMOS (non-public)
- FLASH
- PPM
- TITAN
- VAC
- VH-1
- ZEUS

Index

- accuracy, 24
- advection, 15
- anti-diffusion, 31
- artificial viscosity, 30, 43

- B** , 11
- boundary conditions, 7, 25
 - periodic, 25
- Burgers' equation, 38
 - conservation form, 38
 - integral form, 38
 - quasi-linear form, 38

- c , 14
- CFL condition, 24, 32
- characteristic, 16
- characteristic curve, 16
- characteristic form, 13
- characteristics, 25
- compression wave, 38
- conservation form, 7, 13, 22
 - Burgers' equation, 38
- conserved variables, 8
- consistency, 24
- consistent, 24
- control volume, 20
- convergence, 24
- Courant number, 32
- Courant-Friedrichs-Levy condition, 24

- density, 57
- differential form, 7, 10
- diffusion, 31
- dimensional splitting, 54
- directional splitting, 54
- dispersion, 32
- dispersion relation, 32
- domain of dependence, 23, 46
- dynamic viscosity, 10

- e_i , 57
- eigenvalue, 14
- e_{ik} , 57
- e_{ikb} , 11, 57
- e_{ikg} , 10, 57
- energy
 - internal, 57
 - total, 10, 11, 57
- entropy condition, 40
 - violation of, 43
- entropy fix, 44
- equation
 - Burgers', 38
 - heat, 17
 - linear advection, 15
 - modified, 31
- equation of state, 7
- Euler scheme
 - for hyperbolic PDE, 19, 26
 - for ODE, 16
 - for parabolic PDE, 18
- expansion wave, 39

- finite differences, 20
- finite elements, 20
- finite volumes, 20
- flux-limiter, 34
- flux-splitting, 41
- forward-time central-space, 26
- F_{rad} , 11
- frequency, 57
- FTCS, 26

- Gauß theorem, 10
- ghost cells, 25
- Gibb's phenomenon, 29
- Godunov-type scheme, 25, 44, 48
- gravitational potential, 10
- grid, 21, 37
 - Eulerian, 21
 - Lagrangian, 21

- heat equation, 17
- hyperbolic, 13, 24

- \bar{l} , 57
- implicit, 26
- initial conditions, 7
- integral form, 9, 21
 - Burgers' equation, 38
- intensity, 57
- internal energy, 57
- I_ν , 57

- Jacobian, 13

- Lax's equivalence theorem, 24
- linear advection equation, 15
 - solution, 21
 - solution of, 15

- magnetic field, 11
- magneto-hydrodynamics, 11
- mass density, 57
- Maxwell stress tensor, 11
- MHD, 11
- modified equation, 31

- MUSCL, 48
- \hat{n} , 57
- normal vector, 57
- ν , 57
- number Courant, 32
- ODE, 16
- operator splitting
 - Godunov, 53
 - Strang, 53
- order, 24
- ordinary differential equation, 16
- P , 57
- parabolic, 17
- partial differential equation, 7
- PDE, 7
 - hyperbolic, 13, 24
 - parabolic, 17
- Φ , 10
- piecewise linear method, 34
- PLM, 34
- PPM, 48
- \bar{P}_{rad} , 11
- pressure, 46, 57
- primitive variables, 8
- quasi-linear
 - Burgers' equation, 38
 - system of PDEs, 13
- radiation pressure, 11
- radiative energy flux, 11
- range of influence, 23
- Rankine-Hugoniot condition
 - for Euler equation, 47
 - for scalar equation, 39
- rarefaction wave, 39
 - transonic, 41
- Reconstruct-Solve-Average, 25, 33, 48
- reconstruction, 33
 - of finite difference scheme, 20
 - of finite volume scheme, 20
 - piecewise parabolic, 36
 - properties of, 33
- restriction
 - of finite difference scheme, 20
 - of finite volume scheme, 20
- ρ , 57
- ρe_i , 57
- Riemann problem, 41
- Riemann solver, 44
- RSA, 25, 33, 48
- scheme
 - 1st order upwind method, 27
 - Beam-Warming, 28
 - slope, 34
 - BTCS, 26
 - CIR, 41
 - Courant-Isaacson-Rees, 41
 - donor cell, 25, 27
 - slope, 34
 - slope-limiter, 34
 - explicit, 23
 - Fromm, 29
 - slope, 34
 - FTBS, 27, 41
 - FTCS, 26, 32
 - FTFS, 27
 - Godunov type, 48
 - Godunov-type, 25, 44, 48
 - implicit, 23, 26
 - Lax-Friedrichs, 28
 - Lax-Wendroff, 28
 - slope, 34
 - slope-limiter, 34
 - leapfrog, 23
 - naive, 26, 32
 - non-conservative, 41
 - PLM, 34–36
 - PPM, 36
 - WENO, 36
- shock, 38
- shock capturing, 42
- shock speed, 39
- shock tracking, 42
- shock wave, 41
- similarity solution, 40
- slope-limiter, 34
 - Minmod, 34
 - Superbee, 36
 - vanLeer, 35
- Smoothed Particle Hydrodynamics, 20
- Sod shock tube, 47
- sound speed, 14
- source term, 10
- spectral methods, 20
- SPH, 20
- stability, 24
 - of ODE, 16
 - of parabolic PDE, 18
- stencil, 23
- stencil diagram, 23
- \bar{T}_{mag} , 11
- total energy, 10, 11, 57
- total variation, 33
- Total Variation Diminishing, 33

- transonic rarefaction wave, 41
- truncation error, 24
- TVD property, 33

- unity tensor, 57
- unstable
 - unconditionally, 32
- upwind, 25
- upwind index, 44
- upwinding, 27

- v , 57
- vanishing viscosity, 38
- velocity, 57
- viscosity, 10
 - artificial, 43
 - artificial, 30
 - dynamic, 10
 - numerical, 32

- weak solution, 21, 38